NASA TECHNICAL MEMORANDUM

NASA TM X-1061

NASA TM X-1061

N65-23830
(ACCESSION NUMBER)
24
(PAGES)
(THRU)
1
(CODE)
32
(CATEGORY)
FACILITY FORM 602
(NASA CR OR TMX OR AD NUMBER)

OTS PRICE(S) $
Hard copy (HC) $2.00
Microfiche (MF) .50

SOME DESIGN CONSIDERATIONS FOR SPIN-STABILIZED SATELLITES WITH RIGID EXPANDABLE STRUCTURES

by Robert H. Johns, Reeves P. Cochran, and David A. Spera

Lewis Research Center
Cleveland, Ohio

NATIONAL AERONAUTICS AND SPACE ADMINISTRATION • WASHINGTON, D. C. • MAY 1965

NASA TM X-1061

SOME DESIGN CONSIDERATIONS FOR SPIN-STABILIZED SATELLITES WITH RIGID EXPANDABLE STRUCTURES

By Robert H. Johns, Reeves P. Cochran, and David A. Spera

Lewis Research Center
Cleveland, Ohio

NATIONAL AERONAUTICS AND SPACE ADMINISTRATION

For sale by the Clearinghouse for Federal Scientific and Technical Information
Springfield, Virginia 22151 – Price $2.00

SOME DESIGN CONSIDERATIONS FOR SPIN-STABILIZED SATELLITES WITH RIGID EXPANDABLE STRUCTURES

by Robert H. Johns, Reeves P. Cochran, and David A. Spera

Lewis Research Center

SUMMARY

23830

Large oriented surface areas are required for some spacecraft applications such as space radiators, solar collectors, and micrometeoroid penetration experiments. Obtaining these large areas necessitates the use of expandable structures that can be contained in the payload envelopes of launch vehicles. To explore the problems of stowage and deployment of such expandable structures with rigid plane surfaces, a sample spacecraft mission of a micrometeoroid penetration survey was considered. Variations in the spin-axis attitude of a spin-stabilized spacecraft in several 400-mile circular orbits of the Earth also were determined.

Two types of expandable structures, wrap-around wings and folding umbrellas, were considered for the sample mission. Of these two types, the folding umbrella was the better choice because of its inherent stability about the original spin axis, smaller maximum dimension for a given exposed surface area, and more positively controlled deployment.

Attitude studies that considered only the effects of gravity gradient torque and Earth oblateness on the precession of the spin axis of the umbrella package were made for orbits in several planes. A polar orbit with the spin axis either parallel or perpendicular to the orbital plane resulted in an essentially stable attitude of the package. An equatorial orbit with the spin axis parallel to the orbital plane resulted in a relatively stable attitude that could approximate the direction of the Earth's orbital velocity vector. The rate of spin affected the rate of axis precession in all orbits considered but did not affect the magnitude of deviation from the initial orientation for polar and equatorial orbits.

AUTHOR 1

INTRODUCTION

Some spacecraft systems require oriented surfaces of large area for uses such as solar-cell arrays, space radiators, and meteoroid penetration experiments. Volume restrictions imposed by most launch vehicles necessitate the use

of erectable or expandable structures to obtain these large areas because the configuration of the package in orbit cannot be fitted directly into the payload envelope of the launch vehicle. In some cases, sections of the displayed area must remain essentially rigid in both the stowed and deployed conditions. This study of expandable satellite packages explores some of the problems of stowage and deployment of rigid plane surfaces and considers longtime attitude variations of spin-stabilized satellites.

Expandable structures have been used in several spacecraft that are now in orbit around the Earth, but these have been either of the inflatable type (such as the balloons for Echo I and Echo II) or of the relatively small rigid-panel type (such as the solar-cell arrays for Explorer XII and others). Deployment of large rigid panels to form a segmented parabolic reflector for the proposed solar-energy converter Sunflower has been described in reference 1. These deployment techniques are not necessarily satisfactory for other applications that may require larger areas, more stringent volume requirements on the folded array, or smaller maximum dimensions for a given area to facilitate ground testing in space-environment facilities.

Orientation of the displayed area in a particular direction may be required for certain types of satellite missions. Spin stabilization offers a simple way to establish an original orientation of the satellite and provides some degree of attitude stability. The orientation of a spinning body in orbit about the Earth is affected by many phenomena, however, such as oblateness of the Earth, gravity gradient torque, magnetic torques, and nature of the orbit. Reference 2 provides a method for determining the effect of gravity gradient torque and Earth oblateness on the spin-axis attitude of an Earth satellite in a circular orbit. These two factors are believed to account for most of the perturbations in satellite attitude for most of the orbits of immediate interest.

The study herein reported investigates two new stowage and deployment methods for expandable satellite packages having plane segments. For the purpose of this study, a sample mission and launch vehicle were chosen in order to impose some physical limits on the preliminary design considerations for these expandable packages. The sample mission was a micrometeoroid penetration flux-rate survey made in a 400-mile circular orbit of the Earth. The assumed launch vehicle was the Thor-Delta with a maximum payload capacity of about 750 pounds (for the 400-mile circular orbit considered here) and with a payload envelope that was essentially annular in cross section. The two stowage and deployment methods investigated were wrap-around wings and folding umbrellas. The general design and nature of deployment for both methods are discussed briefly. Some of the forces involved in deployment were evaluated for the umbrella-type expandable satellite package. In addition, variations in the spin-axis attitude were calculated for a spin-stabilized umbrella satellite in several different 400-mile circular orbits of the Earth and for several spin rates.

DESIGNS OF EXPANDABLE STRUCTURES CONSIDERED

To illustrate some preliminary design considerations for expandable spin-

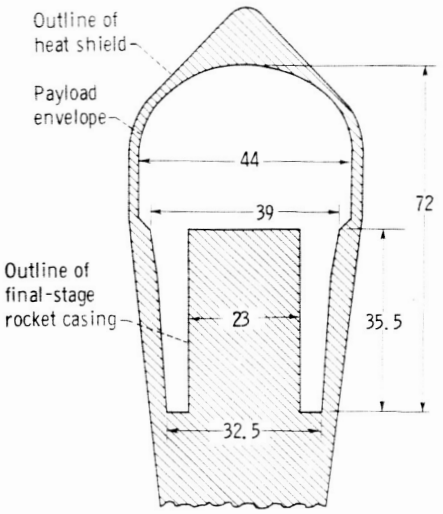

Figure 1. - Approximate dimensions of payload envelope considered in design study of expandable satellite packages. All dimensions are in inches.

stabilized satellite packages having rigid panel segments, a study was made of two basically different methods for stowing and deploying such structures. The general dimensions of the payload envelope of the launch vehicle considered in this study are shown in figure 1. One of the stowage and deployment methods studied utilizes a pair of wings wrapped around the final-stage rocket casing. The other method employs a folded umbrella that surrounds the final-stage rocket casing. These two methods are described in the following paragraphs. Although the designs presented herein are proposed specifically for the sample mission in which the Thor-Delta launch vehicle is used, the design principles can be used in a number of applications where the need arises for deployment of large surface areas in the space environment.

Wrap-Around Wing

One method of stowing a thin structure of large surface area in the essentially annular payload envelope of the launch vehicle (fig. 1) is to wrap the surfaces around the in-

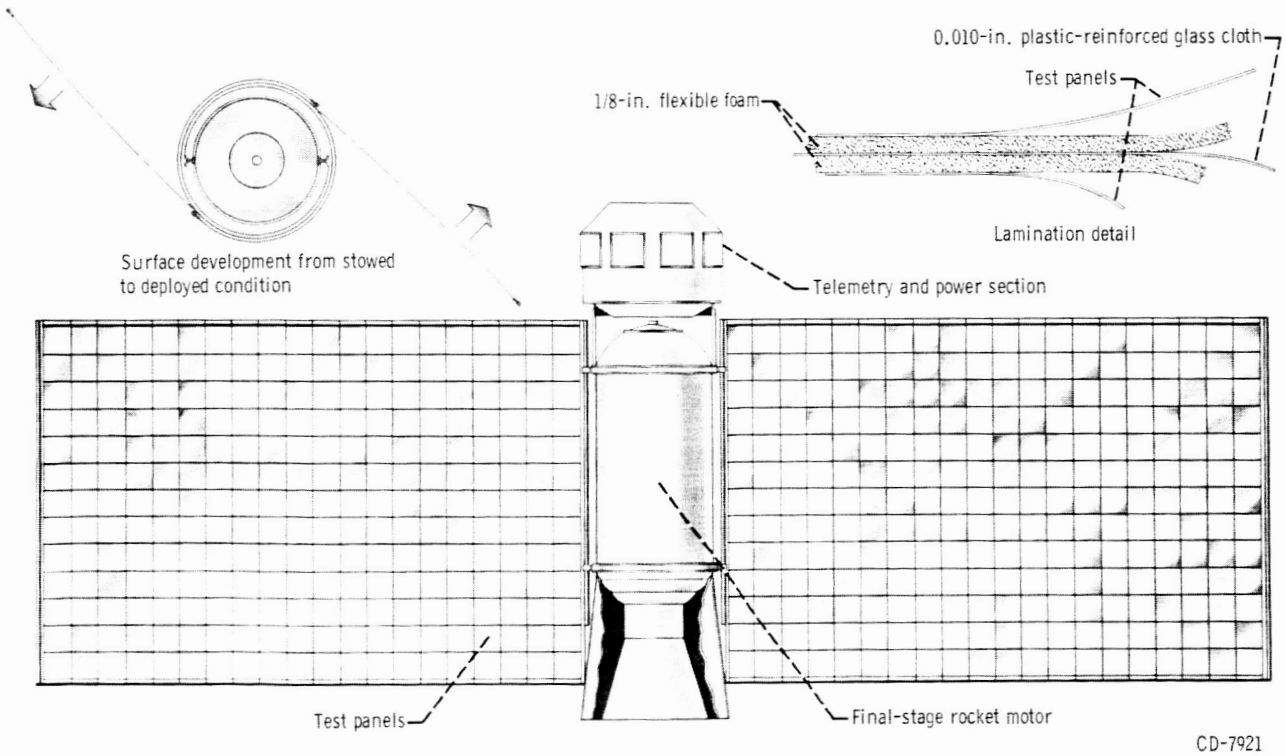

Figure 2. - Rug-type wrap-around wings as expandable structure for satellite package.

ner cylinder of the envelope. If a flexible base can be used for mounting the components to be displayed, the wrapping can be compactly placed next to the cylinder. If the base must be rigid and flat, the area can be segmented and wrapped polygon fashion about the inner cylinder. Examples of these two design concepts are now described.

Rug-type wrap-around wing. - Figure 2 shows a rug-type wrap-around-wing design for stowing an expandable structure with large surface area. A flexible lamination of glass cloth and foamed plastic sheets forms the base for the test panels. The test panels must either be flexible enough to conform to the cylindrical contour, or must be subdivided into small segments that will conform approximately to this contour. The deployed area forms two wings mounted diametrically opposite each other on the final rocket stage. In the stowed condition these wings are wrapped compactly around the rocket stage in overlapping layers. Deployment of the structure is accomplished by utilizing a portion of the spin energy imparted to the final stage for stability. As the wings unfold, the moment of inertia of the package increases, and the spin velocity correspondingly decreases in compliance with the principle of conservation of moment of momentum. Some form of restraining device is required

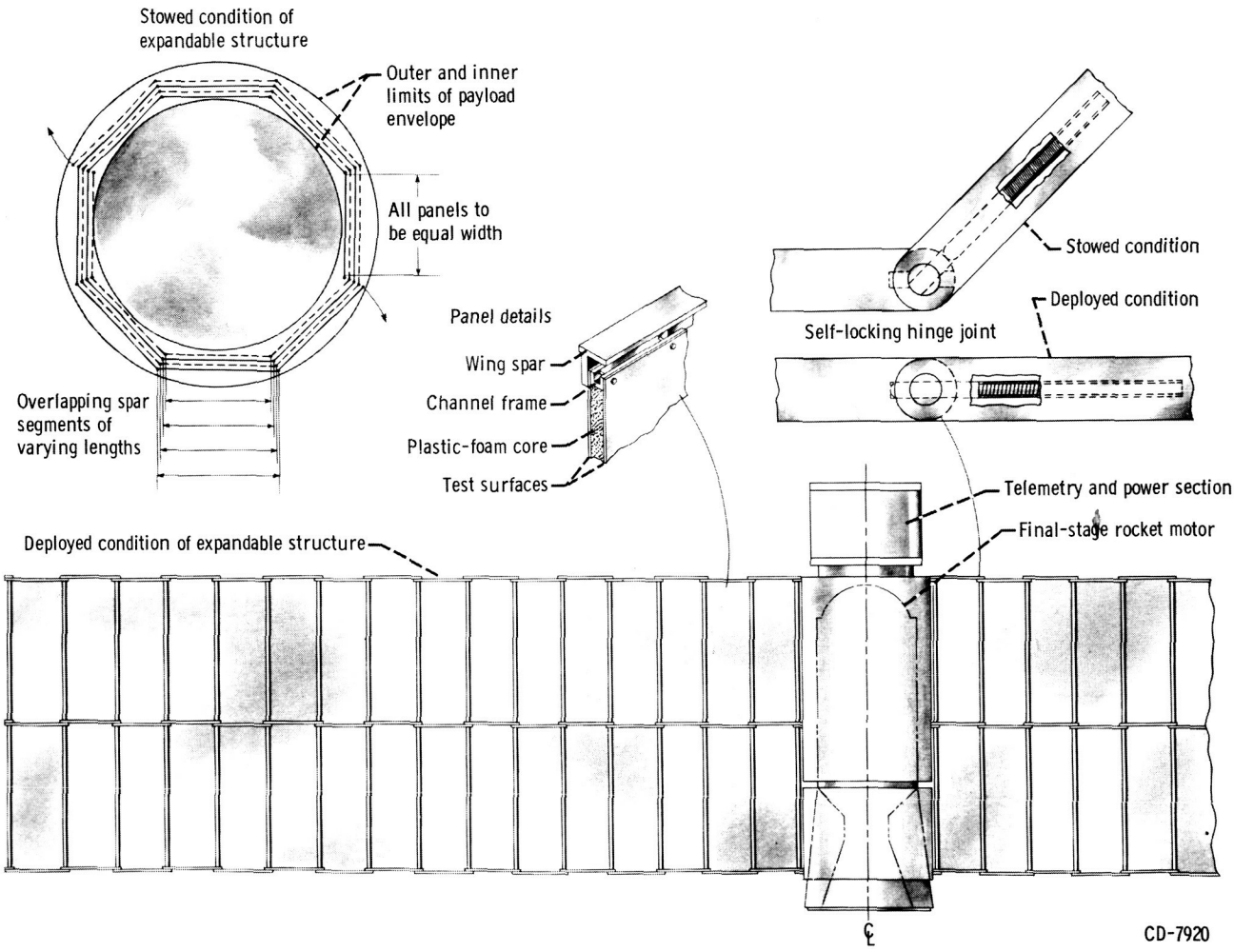

Figure 3. - Segmented or hinged wrap-around wings as expandable structure for satellite package.

to absorb gradually any excess energy in order to permit suitable unfolding of the wings and to prevent excessive oscillation of the wings in the extended position.

The rug-type wrap-around-wing design achieves very economical use of the payload-envelope volume. Large areas are possible with this type of design by using long wing spans (within the limits of payload volume and weight restrictions). These large wing spans, however, mean, among other things, longer instrument leads to the components located on the wings and more difficulty in ground testing the package in environmental facilities.

Segmented or hinged-type wrap-around wing. - For applications where the segments of the structure to be deployed must remain as plane surfaces at all times, a scheme like the one shown in figure 3 can be used for the wrap-around wings. Each wing is subdivided into segments that are hinged to each other. The lengths of the segments of the wing spars increase from the rocket stage outward so that the wings can be wrapped in overlapping layers around the inner cylinder of the payload envelope. An octagonal pattern is shown in figure 3 as being a good compromise between loss of payload volume due to dead space in the annular stowage area and number of hinge joints.

The individual segments of the wings consist of rigid panels of a composite sandwich construction and links of the main support arms or spars of the wing. The panels are fastened to the spars and can be removed easily for repair or replacement. As noted in figure 3, the size of the panels used in this example is the same for all segments of the wing; the differences in segment lengths are in the lengths of the wing-spar links to which the panels are mounted. In this way, a single basic panel pattern can be used for all locations on the wings, and a large inventory of various size panels can thus be avoided. This system involves some loss in exposed area for a given wing span, but the fabrication and servicing of the package are greatly simplified.

The hinge joints (fig. 3) are equipped with self-locking spring-loaded pins to hold the segments in line with each other after deployment. Some additional design details for controlling deployment, which would probably be required but are not shown on the figure, are (1) a method of locking each panel in the folded position until the panel outboard of it has been unfolded and locked in the deployed position, and (2) a restraining device to absorb some of the energy during deployment to prevent the final torque on the base hinge joint from being prohibitive at the conclusion of deployment.

As in the case of the rug-type wrap-around-wing design, a large wing area can be obtained with the hinged-type wrap-around-wing package by using a long wingspan if payload weight and volume limitations permit. The same disadvantages of long wingspans apply here as were noted previously for the rug-type wrap-around-wing design.

Tumbling of wrap-around wing. - A spinning body seeks the mode of least energy, which is rotation about the axis with the greatest moment of inertia. Because the moments of inertia of the deployed wrap-around-wing designs shown in figures 2 and 3 are greater about the axes normal to the deployed surface (spin axis in fig. 4(c)) than about the longitudinal axis (spin axis in

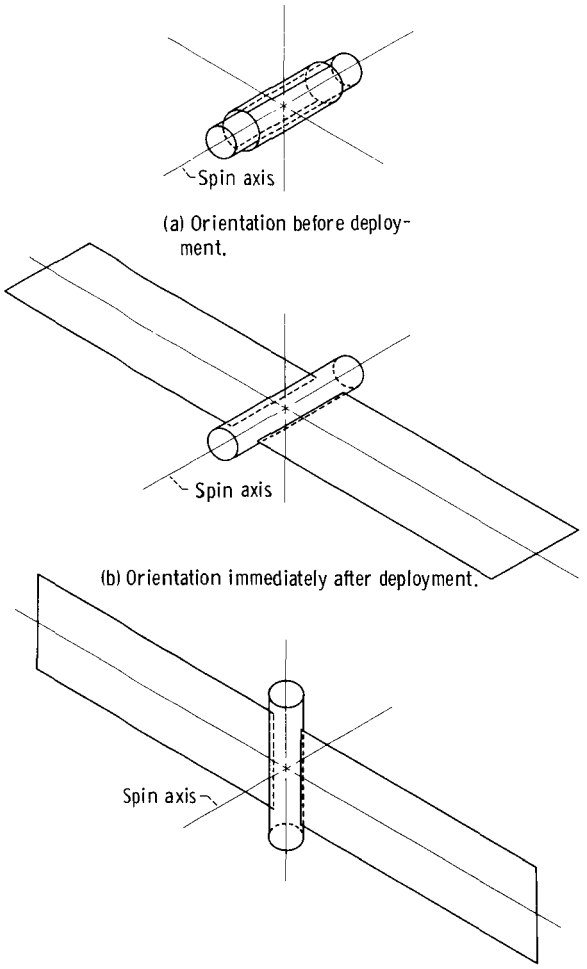

(a) Orientation before deployment.

(b) Orientation immediately after deployment.

(c) Orientation after tumbling.

Figure 4. - Orientation of spin-stabilized wrap-around-wing satellite package.

fig. 4(a)), the wrap-around-wing designs are not stable about their original spin axis. The spinning package will, therefore, tumble or realine itself so that this normal axis becomes the spin axis (fig. 4). The rate at which this realinement occurs depends on the relative magnitudes of the principal moments of inertia, rate of spin of the package, and the damping characteristics of the satellite. The tumbling rates were not calculated for the proposed designs shown, but the rates could be controlled to some degree with proper redistribution of mass about the various axes and by the amount of damping provided.

For the sample mission discussed in this report, it is desired that the final spin axis be normal to the deployed area so that the surface can be properly oriented for meteoroid penetration study. Therefore, this tumbling of the package is a necessary maneuver to achieve the desired surface orientation for the sample mission. An alternative method of achieving this surface orientation without tumbling is to rotate the wings 90° around the transverse axis through the wing tips immediately after deployment. This can only be accomplished at the expense of greater weight, more complexity, reduced reliability, and loss of payload volume. For other applications, where this tumbling action is not desirable, it can be avoided by despinning the package prior to deployment. A self-contained power supply, however, would then be required to deploy the wings, and the passive attitude control inherent in the spin of the package would be lost.

Umbrella

A second type of expandable configuration for the deployment of rigid panels that can be fitted into the annular space of the payload envelope is an umbrella structure such as shown in figure 5. In the deployed condition, such an umbrella has the form of a circular flat disk with a hole at the center. For stowing, the disk is subdivided into panels with a maximum width dimension such that the disk can be contained within the annular space between the inner cylinder and the outer limits of the payload envelope (fig. 1, p. 3). Support arms equally spaced among the panels provide the necessary mechanism for moving

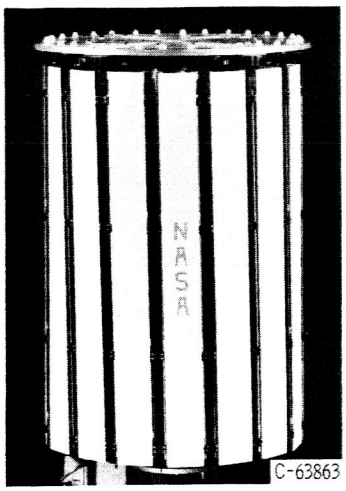

(a) Stowed condition.

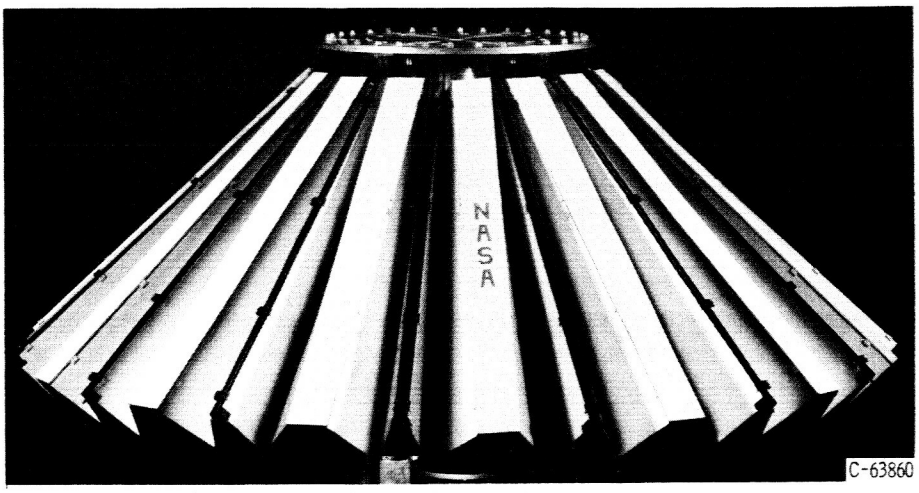

(b) Intermediate condition.

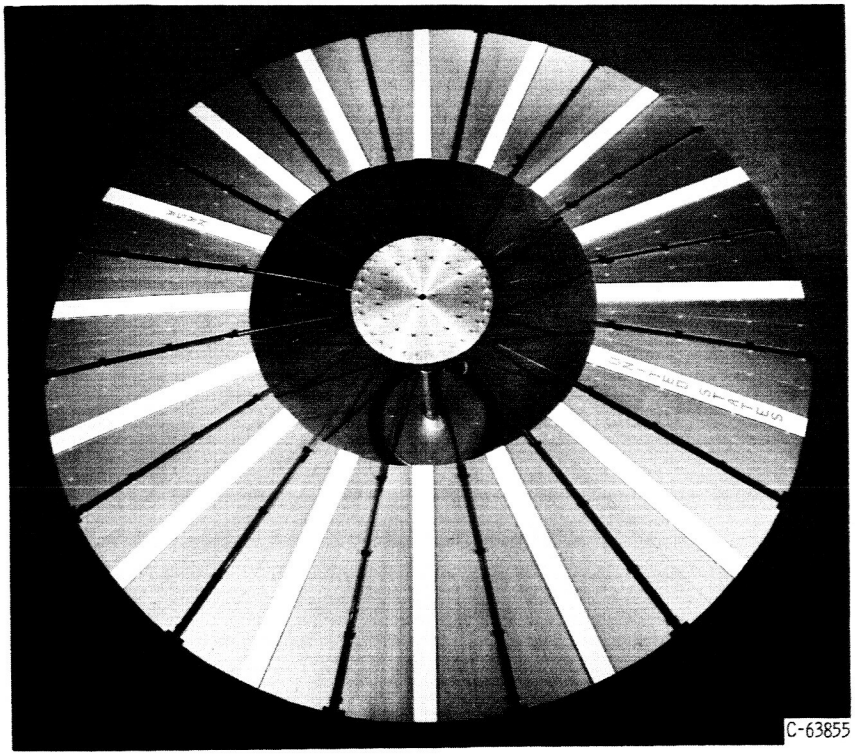

(c) Deployed condition.

Figure 5. - Half-scale working model of telescoping-umbrella package.

the panels from the stowed to the deployed condition and maintain the disk shape after deployment. The length of the panels, which is equal to the difference between the inner and outer radii of the disk, is limited by the longitudinal dimension of the payload envelope. The umbrella configuration uses telescoping (lengthening) support arms to gain additional area. Some of the factors that limit the area that can be obtained with a telescoping-umbrella configuration are the amount of telescoping of the support arms that can be done practically, the necessity of subdividing the disk into numerous panels, and the payload weight and volume limitations.

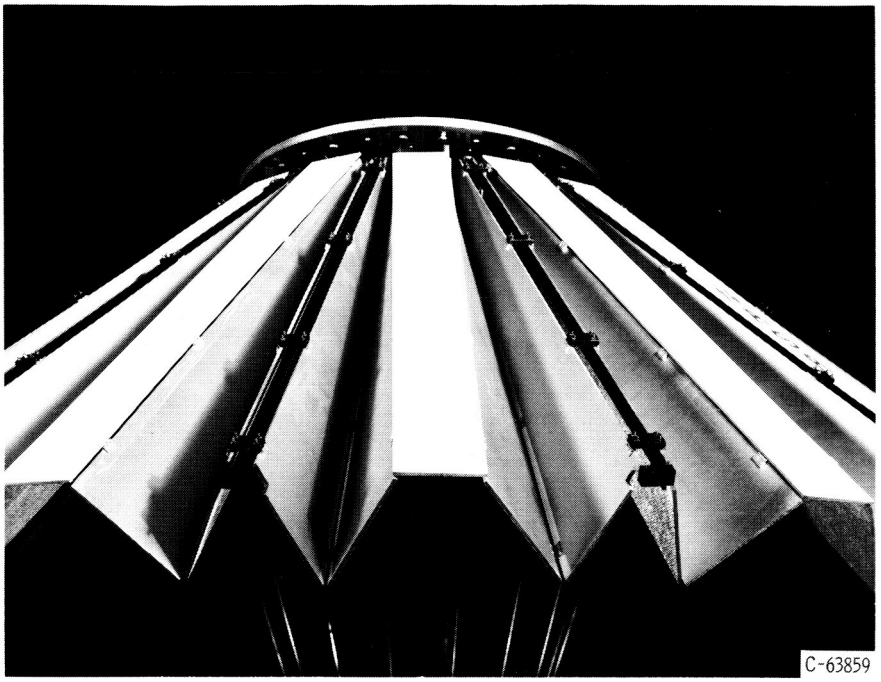

(a) Folding of panel assemblies.

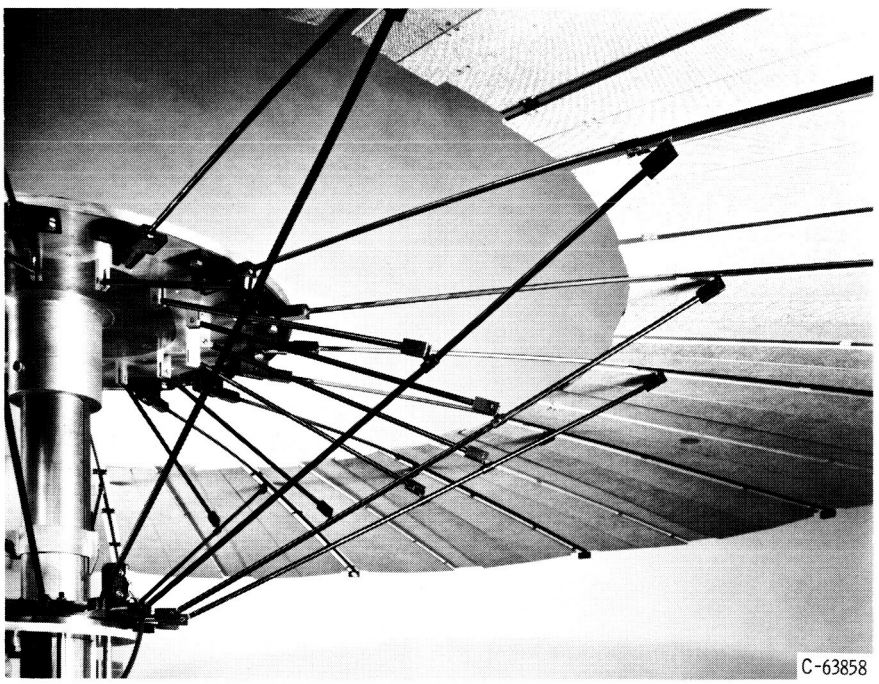

(b) Support linkages.

Figure 6. - Details of half-scale working model of telescoping-umbrella package.

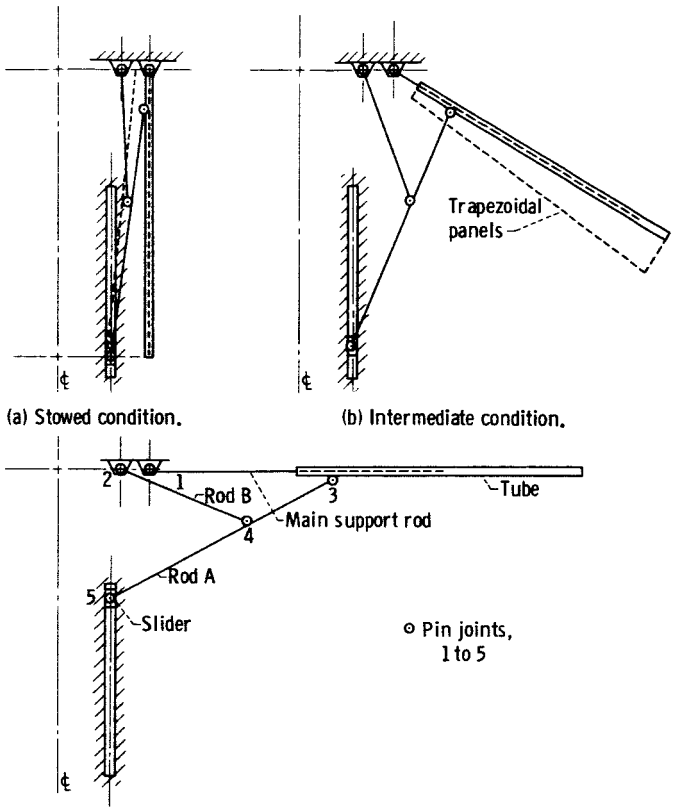

Figure 7. - Schematic diagram of support linkage for telescoping-umbrella package.

For a telescoping-umbrella package, the maximum width dimension for a given deployed area is less than that for the wrap-around designs. This feature makes the testing of the package, full size or as a scaled model, much easier in space-environment chambers. The smaller maximum width dimension of the umbrella package also means shorter lengths of instrument leads to components located on the deployed area than would be possible with the wrap-around designs. Any disturbing forces acting on the package create smaller disturbing moments on the shorter spans of the umbrella-type package than on the longer spans of the wrap-around packages; therefore, this aspect of the attitude problem is less severe with the umbrella package.

Satellite package for sample mission. - Figures 5 to 7 show a working model and a schematic diagram of a telescoping-umbrella satellite package proposed for the sample mission of the present study. In the stowed condition, the package has the shape of a 16-sided right prism (fig. 5(a)), which deploys into a flat annular disk (fig. 5(c)). Sixteen support linkages divide the disk into segments. The method of subdividing these segments into panels that can be stowed in the available payload envelope is seen in figures 5(b), 6(a), and 8.

Each segment of the disk is composed of five panels; the center panel is rectangular, and the other four are trapezoidal (fig. 8). The maximum width of the trapezoidal panels is determined by the radial dimension (difference in radii) of the annular part of the payload envelope. The panels are hinged to each other and thence to the support arms with telescoping rod and tube assemblies. As can be seen in figures 5 and 6, the trapezoidal panels fold inward and are completely hidden from view when the package is in the stowed condition. The rectangular panels make the stowed condition of the package a more rigid configuration that resists distortion at spin-up and reduces the maximum width dimension of the trapezoidal panels. This method of subdividing the segments was also devised to minimize twisting or warping of the panels during deployment of the expandable package.

Figures 7 and 8 show that the panel assemblies are mounted to telescoping rod and tube assemblies on the support linkages. Each of these rod and tube assemblies pivots on a fixed point (point 1) on the stationary part of the

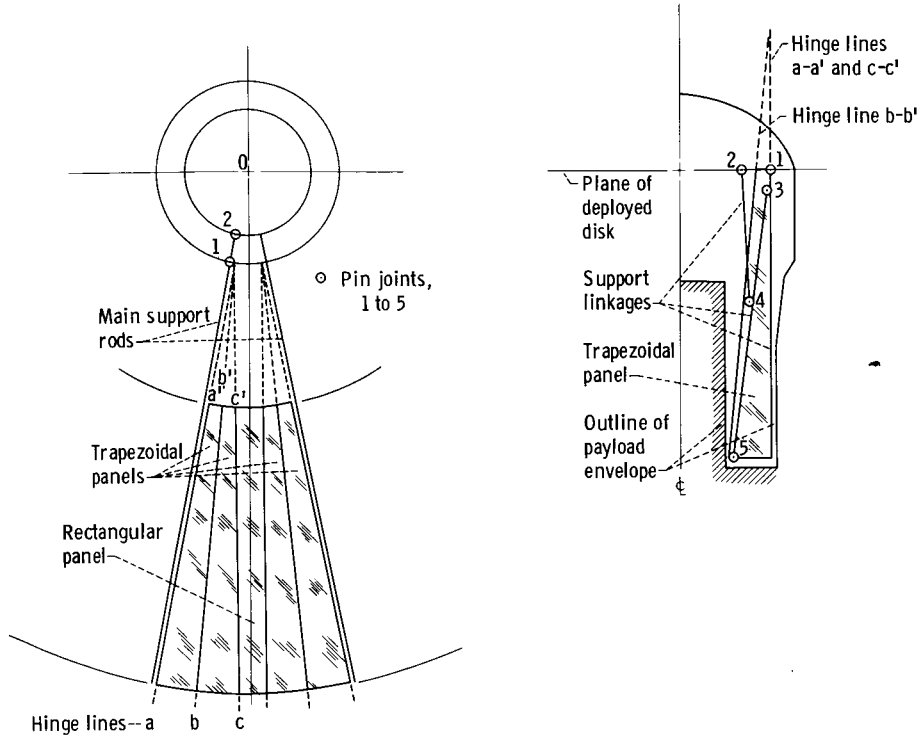

(a) Deployed condition (top view). (b) Stowed condition (longitudinal section).

Figure 8. - Schematic diagram of segment of telescoping-umbrella satellite package (1/16 of total disk).

satellite package. The hinge line between the panel and main support rod is labeled a-a' in figure 8; the hinge lines between panels are labeled b-b' and c-c'.

Details of the support linkages can be seen in figures 6(b) and 7. The support linkages are interconnected through the panels and through common anchors to the stationary part of the package at the linkage pivot point (point 1, figs. 7 and 8) and to a slider (point 5, fig. 7). Each support linkage consists of three rods and a tube. The main support rod is attached at its inboard end (point 1) to the central part of the package. This rod rotates through an angle of 90° during deployment from a position parallel to the longitudinal axis of the satellite to a position normal to the longitudinal axis. The tube slides or telescopes on this rod. In the stowed condition, the inboard end of the tube is against the attachment point of the main support rod (point 1). As the package is deployed, the tube slides outward on this rod (fig. 7). The panels adjacent to the support linkages are attached by hinges to the tubes, and all the panels move outward with the tubes during deployment. The outboard end (point 3) of the second rod (rod A) is attached to the telescoping tube near the inboard end of the tube. The inboard end of rod A (point 5) is attached to a slider. Rod A regulates the opening of the telescoping rod and tube assembly and limits its ultimate travel. Rod B (fig. 7) is attached at its inboard end (point 2) to the central part of the package and at its outboard end to a point (point 4) near the middle of rod A. Rod B helps support rod A and also provides a convenient route for running instrument leads to components located on the panels of the disk. The motion

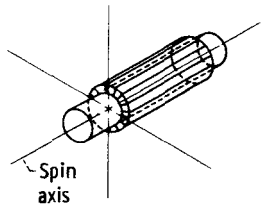

(a) Orientation before deployment.

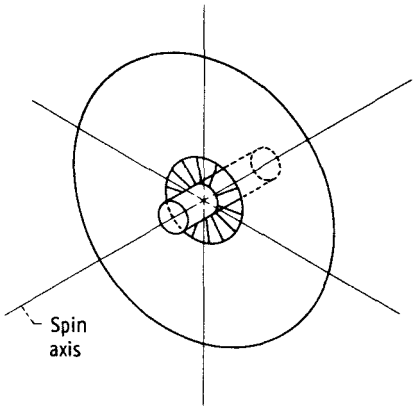

(b) Orientation after deployment.

Figure 9. - Orientation of spin-stabilized umbrella satellite package.

of the support linkage during the deployment process is demonstrated schematically in figure 7.

The feasibility of this design of an expandable structure was demonstrated experimentally by deploying the working model in a free-wheeling spin rig under conditions of Earth gravity and atmospheric drag. It should be pointed out that some of the details of the working model in figures 5 and 6, such as the blocks and pins on the ends of the support linkages, are features of the model only and would not be present on a flight package. Also, the materials and methods of construction used in the model are not necessarily those which would be used in a final design.

Inherent stability of umbrella package. - Because the moment of inertia of the deployed umbrella package is greater about the longitudinal or original spin axis (fig. 9) than about either of the other two principal axes, this spinning mode is the mode of least energy and is, therefore, a stable mode. Unlike the wrap-around-wing designs shown in figures 2 and 3, the umbrella package will continue to spin about its original spin axis. For the sample mission considered here, this is a desirable condition.

DYNAMIC ANALYSIS OF PACKAGE DEPLOYMENT

A spin about the longitudinal axis is applied to the final stage of the Thor-Delta launch vehicle to maintain directional stability. This stabilizing spin is a readily available source of energy for deploying the expandable structure of the proposed umbrella satellite. This type of deployment is referred to herein as spin deployment.

The centrifugal forces resulting from the spinning motion, however, cause undesirable stresses in the various components and joints. In the stowed condition, the effects of the centrifugal forces can be limited by firmly anchoring the folded structure at numerous points to the stationary parts of the package and to the final rocket stage. Once the structure is released for deployment, the effects of these forces are concentrated at a few points. A dynamic analysis of the telescoping-umbrella package is presented in this report to determine the magnitudes of the forces and moments involved. In addition to the dynamic analysis, area comparisons are made for various telescoping-umbrella design concepts.

An analysis was made of the deployment of the telescoping-umbrella package shown schematically in figures 10(a) and (b). Symbols used in the analysis are given in appendix A. The assumptions on which the analysis was based and the

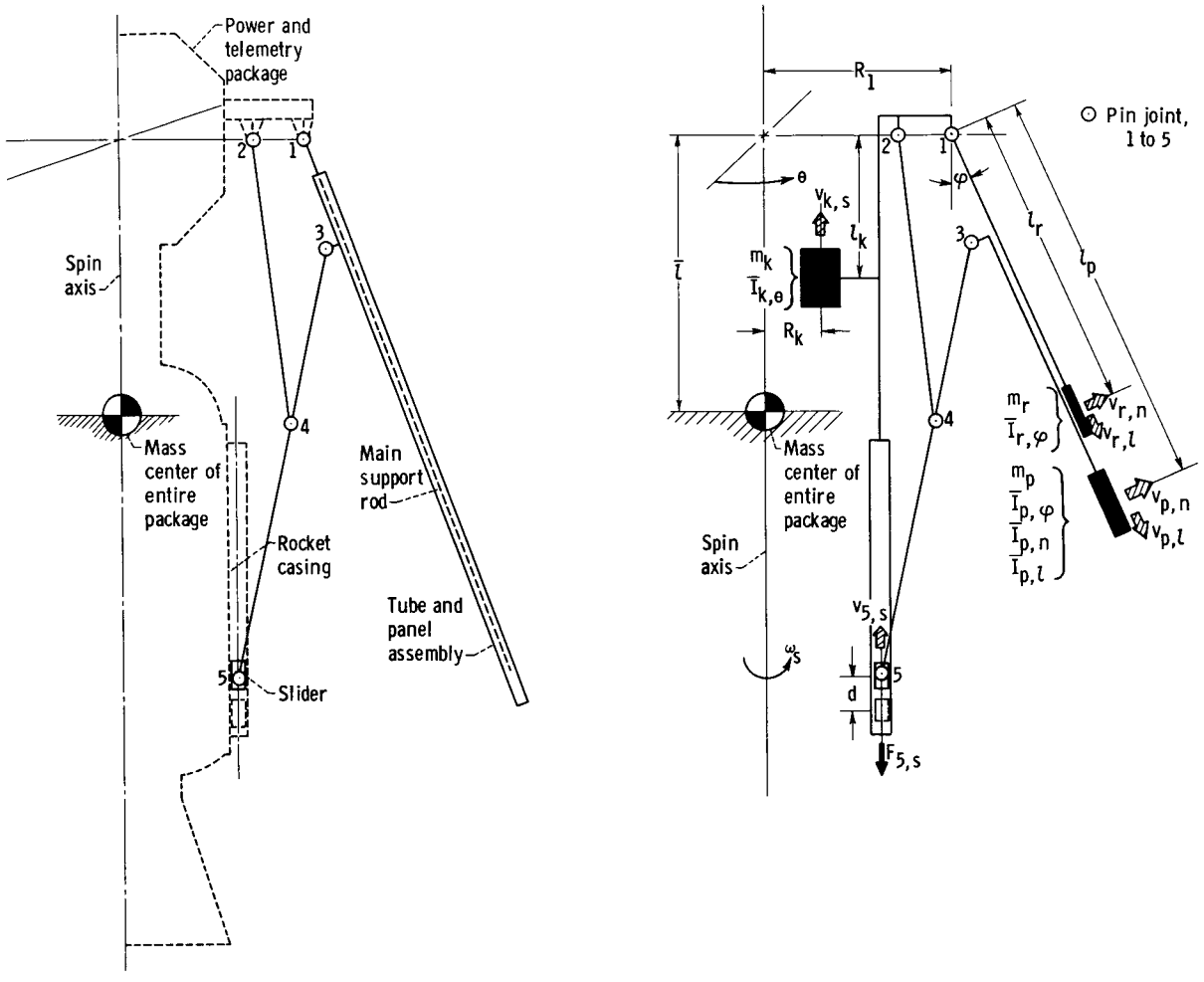

(a) Schematic diagram of umbrella linkage.

(b) Idealized dynamic system.

Figure 10. - Dynamic system used in analysis of restricted spin deployment of telescoping-umbrella satellite.

equations that were developed to describe the dynamics of the package are given in appendix B. By assigning representative numerical values to the geometric and dynamic factors in these equations, illustrative results were obtained. The kinematics of the package are described by the slider travel d and panel extension Δl_p of the mechanism, which are shown in figure 10(c) as functions of the deployment angle φ. An IBM 7094 electronic computer was used to solve the equations.

The spin energy stored in the satellite makes possible a convenient and simple method of accomplishing deployment of an expandable umbrella package. Overstressing of the structure can result, however, if deployment is allowed to progress unrestricted. If the package deployment is restrained, the package spin deceleration $\ddot{\theta}_{neg}$ and the terminal velocity of the support arms $\dot{\varphi}_f$ can be reduced. Therefore, in the analysis, a simple energy absorber such as a hydraulic dashpot was assumed as a retarding mechanism. The retarding force $F_{5,s}$ (fig. 10(b)) of such a mechanism is directly proportional to the linear

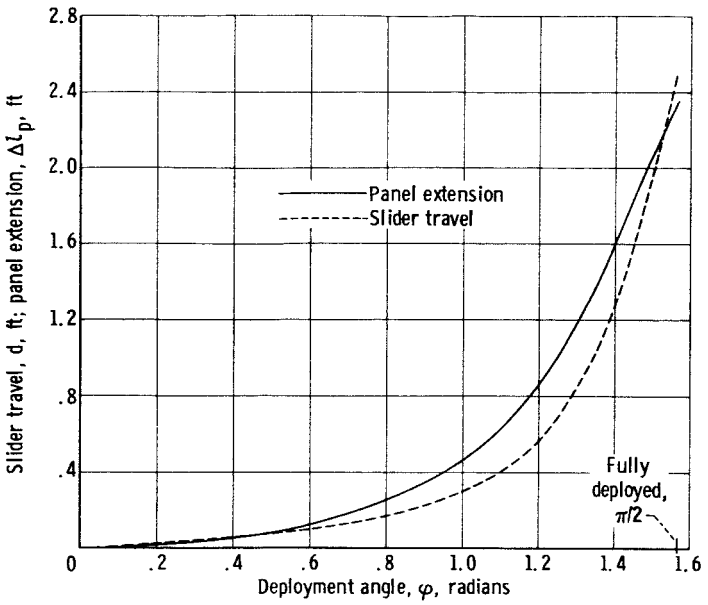

(c) Linkage motion.

Figure 10. - Concluded. Dynamic system used in analysis of restricted spin deployment of telescoping-umbrella satellite.

velocity $\dot{d}$ of the slider. The proportionality factor between the damping force $F_{5,s}$ and the slider velocity $v_{5,s}$ is called the damping coefficient μ. By varying the value of this coefficient results can be obtained over a wide range, from the undamped case ($\mu = 0$) to the fully damped case ($\mu = \infty$).

The fully damped case ($\mu = \infty$) is equivalent to a quasi-static condition in which the restraining force supplied by the damper is sufficient to maintain static equilibrium at any stage of the deployment of the package. From the standpoint of stresses developed in the package structure, the fully damped case is also equivalent to the case where deployment is restrained by an onboard power mechanism that permits a constant, slow rate of deployment.

Some results of the analysis are shown as functions of the damping coefficient μ in figure 11. The results are for the specific design considered herein and for an initial spin velocity of 125 rpm (13.1 radians/sec). Results with similar trends would be obtained, however, for somewhat different mechanisms and for different spin speeds.

One of the major reasons for using the damper is to absorb all excess energy during deployment so that the deployment angular velocity of the support arms $\dot{\varphi}$ is approximately zero at full deployment. This absorption of excess energy is necessary to minimize deformations and stresses in the panels and supporting structure when full deployment is accomplished. It can be seen from figure 11 that this function of the damper is accomplished very well when only a relatively small amount of damping is present. For the particular structure and spin speed analyzed, the final deployment angular velocity $\dot{\varphi}_f$ is approximately zero for a damping coefficient μ of 10 or larger. This means that, for large damping coefficients, all excess energy is dissipated prior to full deployment. Consequently, the last few degrees of opening are accomplished at a $\dot{\varphi}$ of almost zero. For this reason, it might be necessary to have a spring-loaded device, or some other energy source that acts during the last few degrees of motion, to force the support arms into the fully deployed position.

The maximum deployment angular acceleration $\ddot{\varphi}_{max,pos}$ takes place instantly upon unlocking of the stowed configuration. As shown in figure 11, this acceleration is a constant 100.45 radians per second per second and is independent of the damping coefficient μ. This instantaneous acceleration

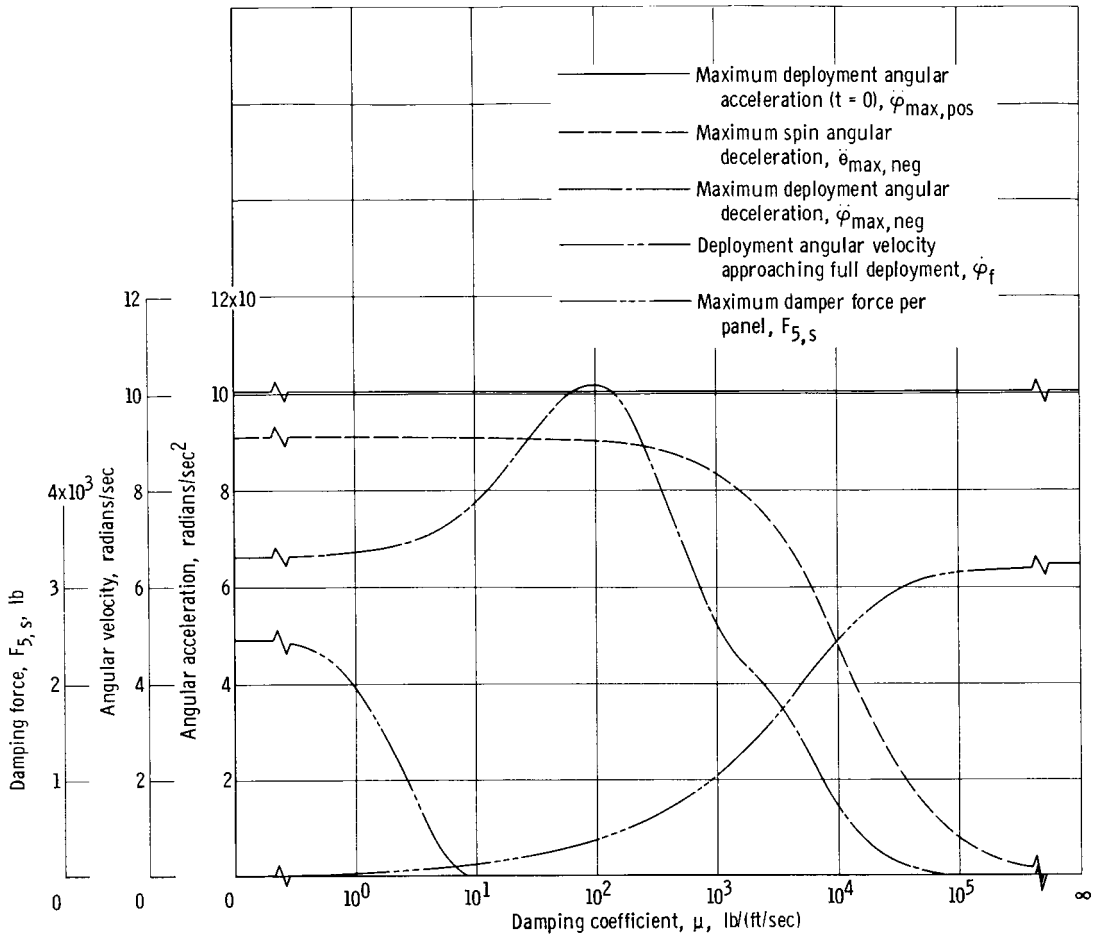

Figure 11. - Effect of damping on dynamics of satellite during deployment. Initial spin rate, 125 rpm.

occurs because the slider must build up some velocity before the linear-velocity damper can retard its motion. At a later time, although still fairly early in the deployment process, the deployment of the arms is slowed down. The maximum deployment angular deceleration $\ddot{\varphi}_{max,neg}$ that occurs at this time is also shown in figure 11. Note that the absolute value of $\ddot{\varphi}_{max,neg}$ peaks for a damping coefficient μ of approximately 100 pounds of damping force per foot per second of slider velocity. For almost all values of μ, $\ddot{\varphi}_{max,pos}$ is greater in absolute value, often considerably so, than $\ddot{\varphi}_{max,neg}$. The bending stresses in the support rods and tubes resulting from the inertial forces induced by these accelerations will likely be a major consideration in the design of the structure.

As is to be expected, the maximum damper force $F_{5,s}$ increases as the damping coefficient μ is increased. For μ approaching infinity, $F_{5,s}$ is about 3250 pounds per panel. Since there are 16 panels in the deployable area, the total damper force for this situation is about 52,000 pounds. This is also the retarding force that would be required of a power mechanism that retards deployment.

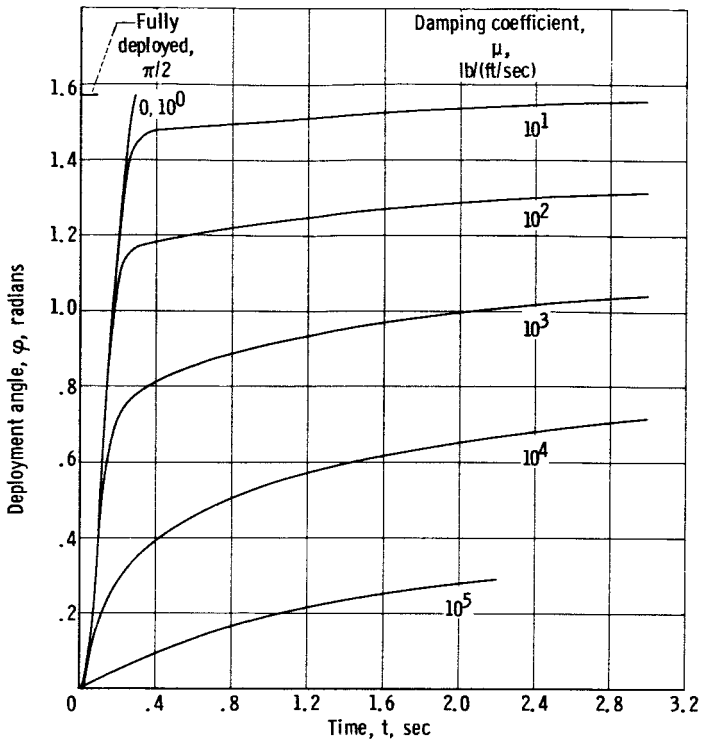

Figure 12. - Variation of deployment angle for umbrella satellite with time for various values of damping coefficient.

As the umbrella satellite package expands from the stowed to the deployed condition, the moment of inertia about the spin axis I_s increases. In accordance with the principle of conservation of moment of momentum, this increase produces a corresponding decrease in the spin angular velocity $\dot{\theta}$ or an angular deceleration $\ddot{\theta}_{neg}$ of the package. The maximum spin angular deceleration $\ddot{\theta}_{max,neg}$ is plotted against μ in figure 11. For small to moderate amounts of damping, $\ddot{\theta}_{max}$ is not much less than for the undamped case. For high damping, $\ddot{\theta}_{max}$ falls off sharply. For the type of design used in the expandable structure of the sample satellite package, the reduction of this $\ddot{\theta}_{max}$ is a most important function of the damper. High-shearing stresses can be induced between the panels of the deploying surface area and the relatively large nondeployable mass by this deceleration. The many segments of the panels and the relatively flexible, lightweight support structure shown in figure 6 (p. 8) cannot withstand large torsional loads. For this structure, it would therefore be necessary to use either a high-coefficient damper or a power mechanism to restrain deployment.

Some partial results of deployment angle φ as a function of time t are shown in figure 12 for various amounts of damping. For no damping, the expandable structure naturally deploys very rapidly, the deployment time being less than 0.3 second. Because of the computer time involved and because most of the dynamic results of interest occur early in the deployment process, total-deployment times and profiles were not obtained for most cases. Note that except for very heavy damping the structure hardly feels the damper until a considerable opening angle has been achieved. The reason for this behavior can be found in figure 10(c). Only about 12 percent of the total slider travel has taken place when about 70 percent of the deployment ($\varphi \approx 1$ radian) has been accomplished. Thus, for light or moderate amounts of damping, the slider velocity and, therefore, the damper force do not build up until late in the deployment process. Hence, for these cases, the early part of the deployment process is very similar to the undamped case. It is true, however, that the total deployment time involved is only seconds or perhaps minutes.

Plots of deployment angular velocity $\dot{\varphi}$, acceleration $\ddot{\varphi}$, spin angular velocity $\dot{\theta}$, and acceleration $\ddot{\theta}$ against deployment angle φ are presented in

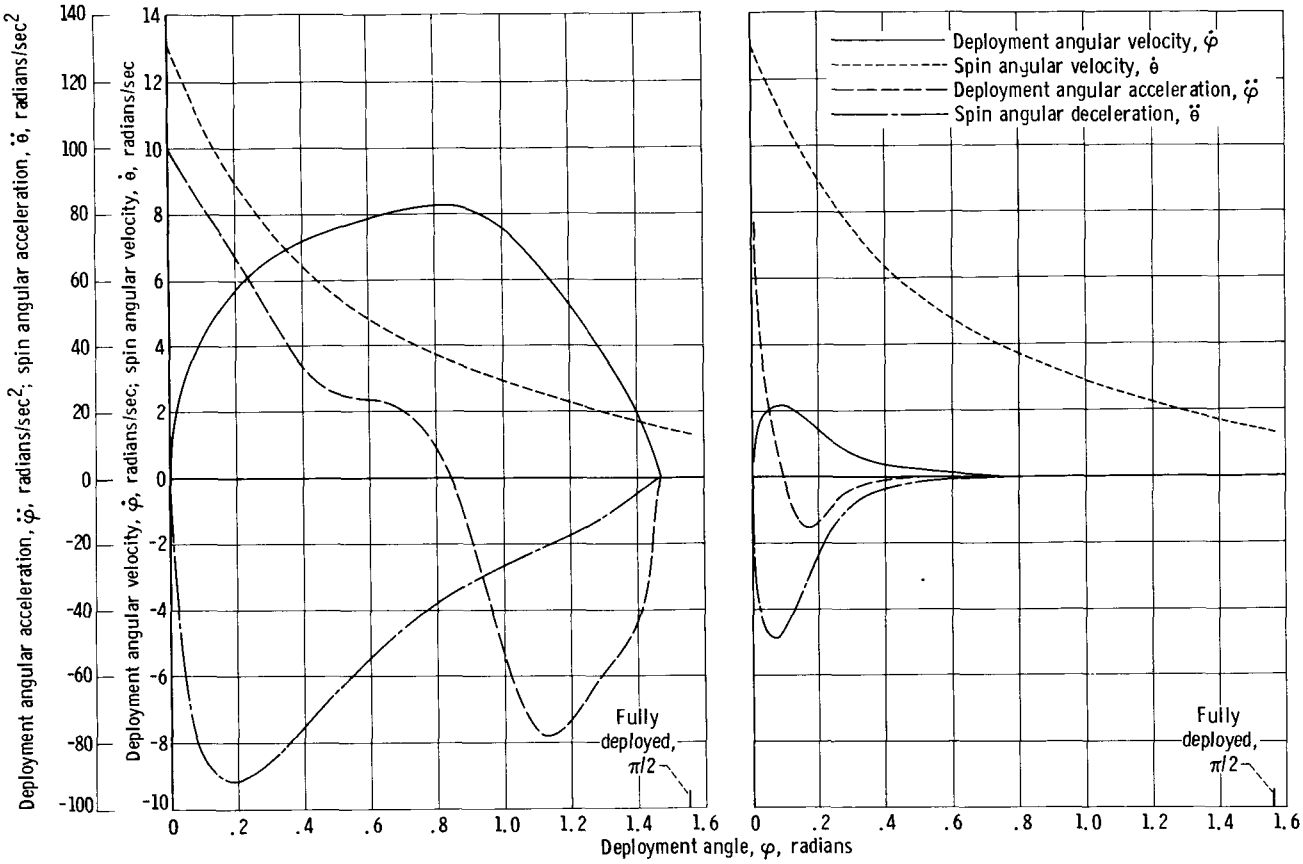

(a) Damping coefficient, 10 pounds per foot per second. (b) Damping coefficient, 10^4 pounds per foot per second.

Figure 13. - Dynamics of satellite deployment as function of deployment angle for two values of damping coefficient.

figure 13 for values of the damping coefficient μ equal to 10 and 10^4 pounds per foot per second. As mentioned previously, the onset rate of spin angular deceleration is very high; this onset rate is associated with a large despin torque that would probably distort severely the structural design shown in figures 5 and 6 (pp. 7 and 8). The reduction in spin angular velocity $\dot{\theta}$ is also shown clearly as a function of deployment angle φ. Correlating figure 13 with figure 12 gives the variation of these parameters with time. From this correlation it can be seen that if the abscissas of figures 13(a) and (b) were time instead of deployment angle, the slopes of the curves would be much steeper, since the region up to 1.47 radians would be severely compressed. From figure 12 this compression is apparent because it takes less than 0.4 second for the first 1.47 radians of deployment, whereas it takes about 3 seconds for the last 0.1 radian for a damping coefficient of 10 pounds per foot per second.

The magnitudes of the dynamic forces involved can be reduced by employing lower initial spin velocities. The initial spin velocity chosen, however, must be commensurate with the requirement of spin stabilization of the final stage of the launch vehicle until injection into orbit. Lower spin velocities mean lower stresses in the package components and permit lighter structural weights. Lower initial spin velocities, however, also mean lower spin velocities for the

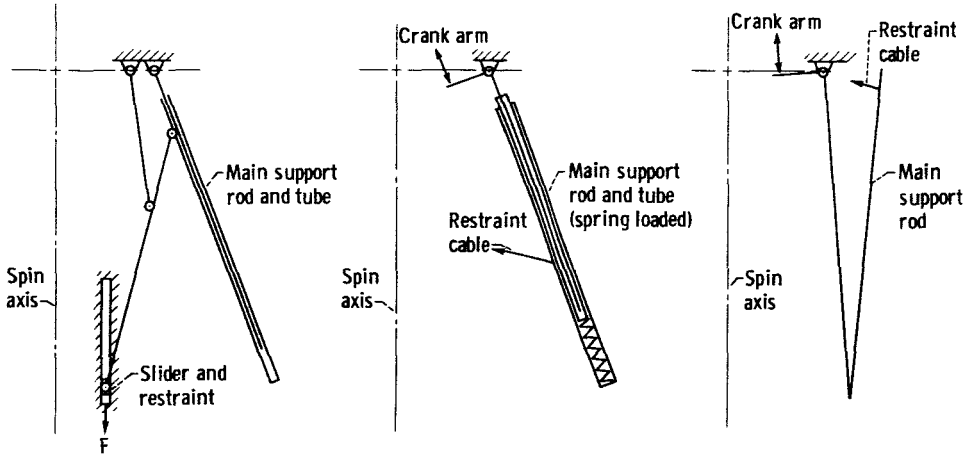

(a) Linkage 1. Maximum area, 200 square feet.

(b) Linkage 2. Maximum area, 310 square feet.

(c) Linkage 3. Maximum area, 285 square feet.

Figure 14. - Area comparison of various linkage concepts for umbrella satellite. (Maximum areas are those possible with these linkages and the Delta payload envelope.

deployed satellite. This condition may not be desirable from the standpoint of attitude stability of the satellite after injection into orbit, as will be discussed in the section SATELLITE ATTITUDE STUDIES.

AREA COMPARISONS OF VARIOUS PACKAGE DESIGN CONCEPTS

The proposed umbrella satellite package is not presumed to be the optimum way to utilize the capabilities of the launch vehicle; it is rather a basic design on which to make a study of the structural problems involved in expandable satellite structures. In this section, two other possible linkage configurations for the telescoping-umbrella package are presented briefly. These two configurations, along with the linkage analyzed in section DYNAMIC ANALYSIS OF PACKAGE DEPLOYMENT (linkage 1), are shown schematically in figure 14. The two new configurations (linkages 2 and 3) differ from linkage 1 in that two points of retarding-force application are used rather than one. One of these retarding forces is provided by a cable restraint, the other by a crank arm. The two forces must be properly synchronized for smooth operation in the deployment of the package. Linkage 2 uses the energy stored in compression springs to assist in the final stages of deployment.

The results of an analysis made on the three linkage configurations to determine the maximum possible deployable area are presented in figure 14. For this analysis, the length of the panels and the number of support arms are assumed to be the same in all cases. For deployed areas greater than 200 square feet, the deployed disk was subdivided into a greater number of panels than shown in figure 5. This was necessary because of space limitations in the annular stowage area of the payload envelope.

The maximum area that can be deployed with linkage 1 for the payload envelope considered is 200 square feet. With the use of a second telescoping tube as in linkage 2, a greater outer diameter and, therefore, a larger area

of 310 square feet (limited by the payload capability of the launch vehicle) can be obtained. The maximum area obtainable with linkage 3 is 285 square feet.

From these brief comparisons of the three linkage configurations, the final design of the satellite package for a mission such as the one considered in this study depends on a number of compromises among factors such as complexity of opening mechanism, weight limitations, and reliability. No attempt has been made here to define an optimum package design or to present a complete survey of possible design concepts. The intent has been to illustrate with general design concepts some of the structural problems involved in the design of an expandable satellite package.

SATELLITE ATTITUDE STUDIES

The sample mission considered in this report is a meteoroid penetration flux-rate survey made in a 400-mile circular orbit of the Earth. The purpose of such a survey would be to determine the number and direction of meteoroid penetrations through various thicknesses of structural sheet materials placed in a near-Earth orbit for a usable lifetime of about 1 year. Reference 3 shows that directional, temporal, and spatial variations exist in the meteoroid population near the Earth, as measured by Earth-based visual and radar surveys. It is therefore desirable that the test specimens in this orbital survey maintain a predetermined spatial orientation or that the change in orientation be determinable so that some measurement of these meteoroid directional variations can be made. For the sample mission, reliance is made on passive attitude control as established by spin stabilization of the final stage. The following discussion considers the effectiveness of such a passive attitude control based on certain simplifying assumptions. For this investigation, active attitude-control systems were not considered.

Factors Affecting Orbit and Satellite Attitude

Among the more important factors affecting the orbit and attitude of an artificial satellite of the Earth are the following:

(1) Solar radiation pressure

(2) Atmospheric drag

(3) Internal energy dissipation

(4) Distribution of mass in satellite

(5) Eddy current torques

(6) Permanent magnetic torques

(7) Induced magnetic torques

(8) Gravity gradient torques

(9) Oblateness of the Earth

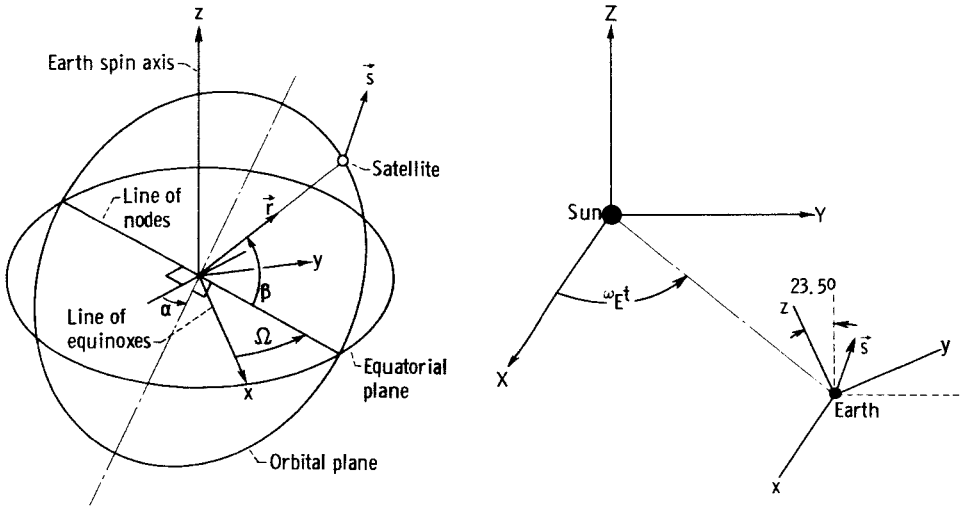

(a) Orbital geometry and geocentric equatorial system.

(b) Heliocentric ecliptic coordinate system and geocentric equatorial coordinate system.

Figure 15. - Orbital geometry and coordinate systems used in satellite attitude studies.

For the orbit altitude used for the sample mission, solar radiation pressure and atmospheric drag can be neglected in comparison with other disturbances (ref. 4). The remaining factors listed, in general, can affect the degree of attitude control maintained by spin stabilization of the satellite package.

The proposed satellite package is not a rigid body and is, in fact, a very flexible body. Consequently, energy considerations are very important. Since energy will be dissipated through the flexible joints, the satellite package will naturally seek the lowest energy level. A spinning body is at its lowest energy level if the axis of maximum moment of inertia is coincident with the axis of spin. Therefore, where possible, it is usually desirable to make the axis of maximum moment of inertia the initial spin axis and thus avoid subsequent orientation changes that involve tumbling of the satellite. In all attitude studies made in this report, it is assumed that spin takes place about the axis of maximum moment of inertia. The symmetrical distribution of the masses of the panels at their relatively large radii makes possible the satisfying of this condition in the umbrella configuration. This was one of the primary reasons for selecting the umbrella configuration instead of the wrap-around-wing design, as noted in the section "Inherent stability of unbrella package." Possible misalinement of the thrust vector, unbalance, and other disturbances may cause the spin axis initially to nutate slightly about the angular momentum vector. Because of the flexibility of the structur, however, energy will be dissipated, and the spin axis will again aline itself with the angular momentum vector.

If a magnetic field is cut by a conductor, a voltage is induced, and a current flows in any closed loop of the conducting material. Thus, eddy current torques would be induced in the proposed satellite package because of the large conducting surfaces spinning in the geomagnetic field of the Earth. Magnetic torques also arise from ferromagnetic material orbiting in the geomagnetic field of the Earth. The eddy current and magnetic torques tend to

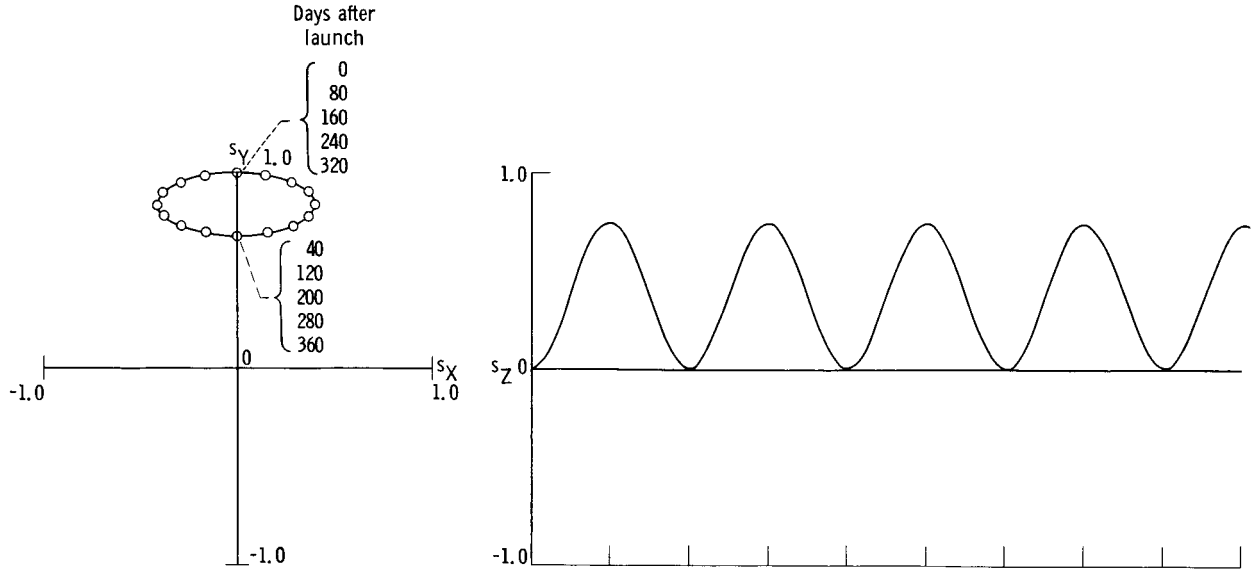

(a) Initial angular position of ascending node, 0^0; spin velocity of satellite, 0.549 radian per second ($k = 1.979 \times 10^{-6}$ radian/sec).

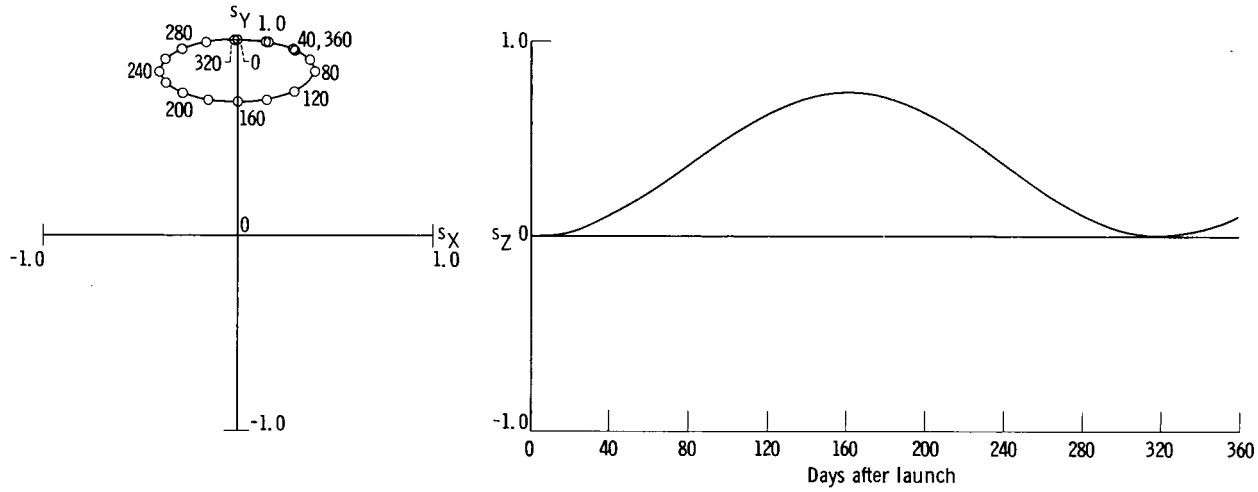

(b) Initial angular position of ascending node, 0^0; spin velocity of satellite, 2.195 radians per second ($k = 0.495 \times 10^{-6}$ radian/sec).

Figure 16. - Precession of unit spin vector for 400-mile polar orbit with spin vector initially parallel to Earth's orbital velocity vector. Moment of inertia about spin axis, 385 slug-feet^2; moment of inertia about transverse axis, 264 slug-feet^2.

despin the satellite, as well as affect its attitude directly, by applying torques about axes other than the spin axis. These torques are difficult to measure or to predict. An independent study indicated that the probable eddy current torques and the magnetic torques (both permanent and induced) were small for the proposed configuration and could be neglected in the preliminary investigation.

Since the gravitational attraction between two masses is inversely proportional to the square of the distance between them, a mass farther from the center of the Earth is attracted with a smaller force than an identical mass closer to the center of the Earth. These differential gravity forces result in a torque that is known as a gravity gradient torque. The oblateness of the Earth produces a gravitational force that does not lie in the orbital plane.

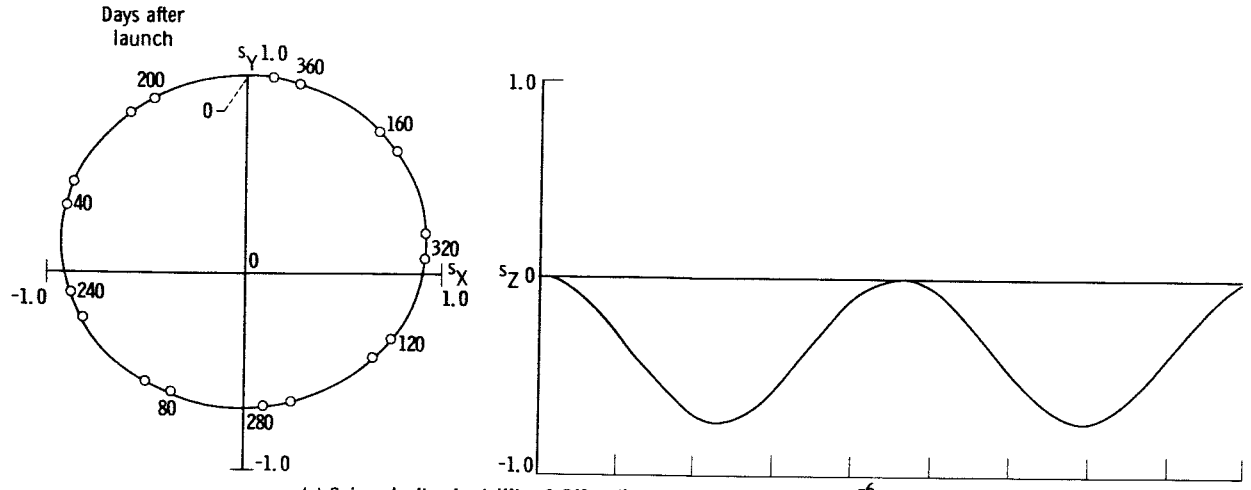

(a) Spin velocity of satellite, 0.549 radian per second ($k = 1.979 \times 10^{-6}$ radian/sec).

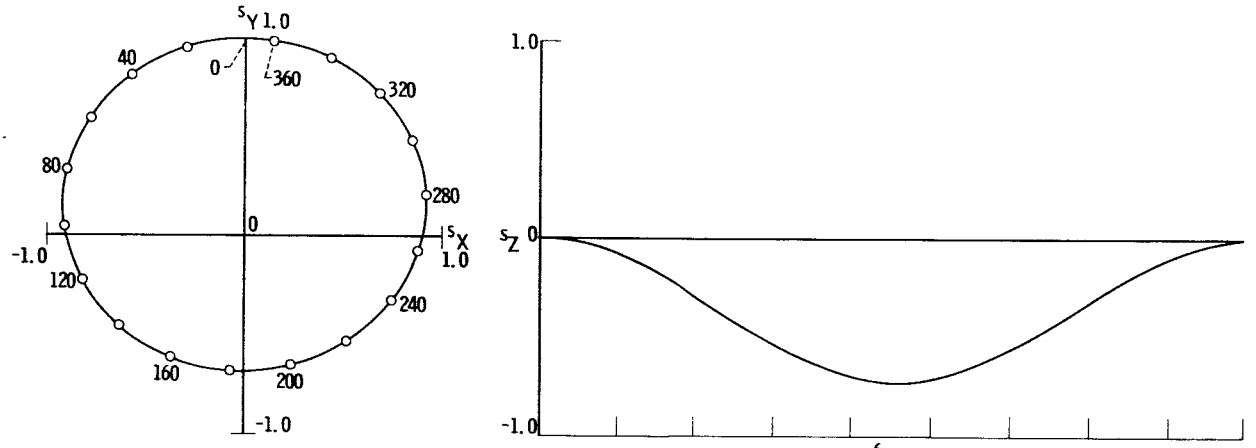

(b) Spin velocity of package, 1.098 radians per second ($k = 0.989 \times 10^{-6}$ radian/sec).

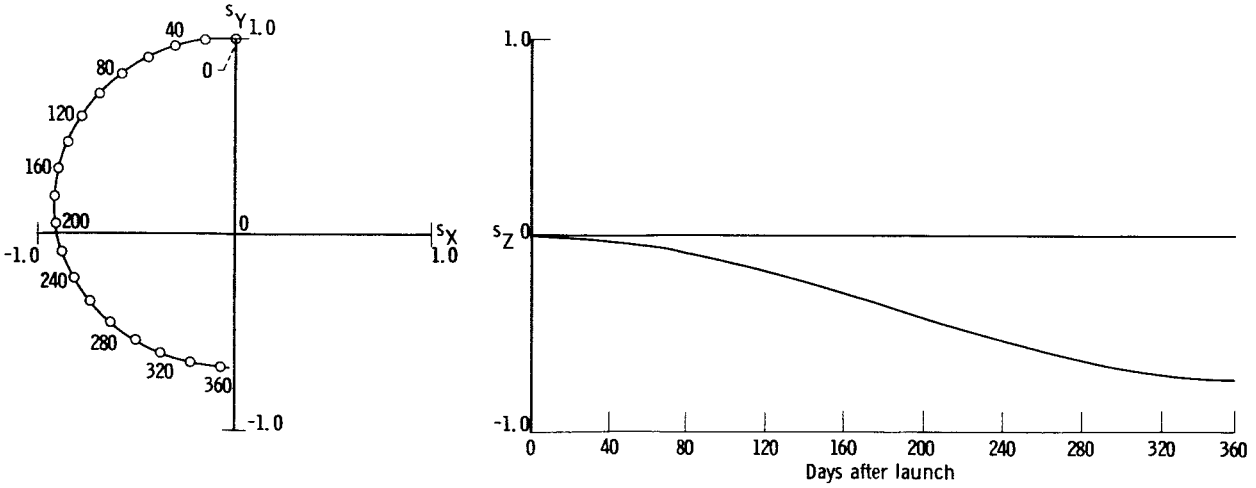

(c) Spin velocity of package, 2.195 radians per second ($k = 0.495 \times 10^{-6}$ radian/sec).

Figure 17. - Precession of unit spin vector for 400-mile equatorial orbit with spin vector initially parallel to Earth's orbital velocity vector. Moment of inertia about spin axis, 385 slug-feet^2; moment of inertia about transverse axis, 264 slug-feet^2.

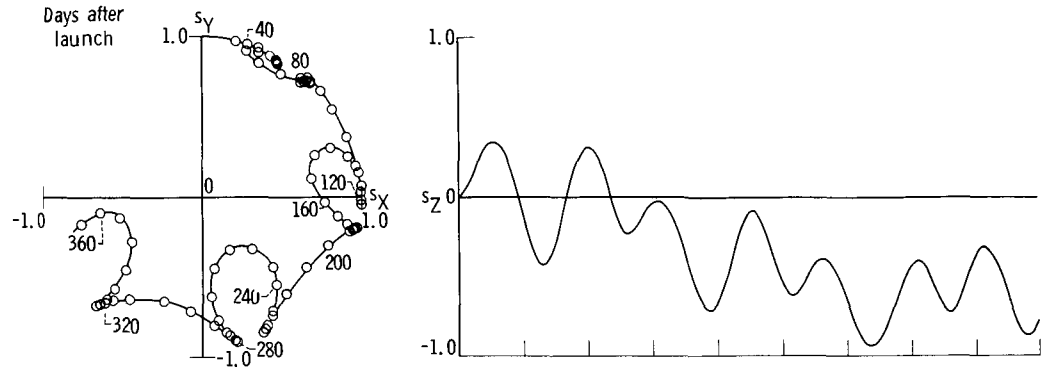

(a) Initial angular position of ascending node, 0^0; spin velocity of satellite, 0.549 radian per second ($k = 1.979 \times 10^{-6}$ radian/sec).

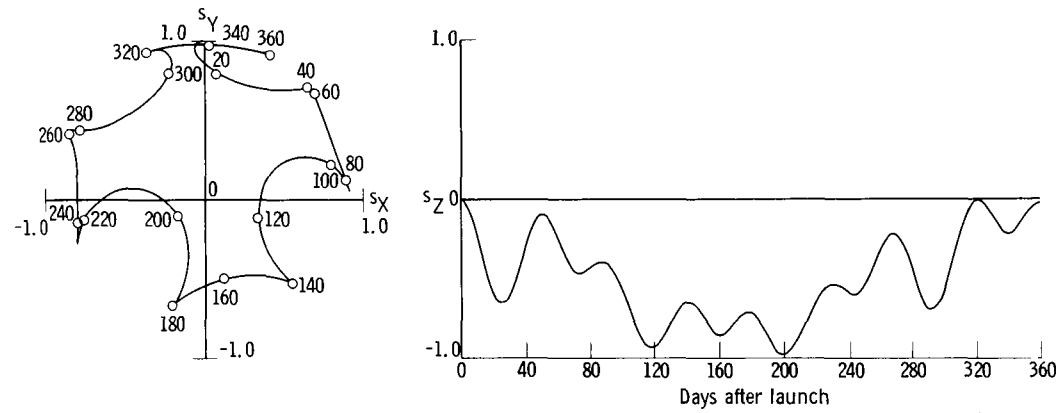

(b) Initial angular position of ascending node, 90^0; spin velocity of satellite, 0.549 radian per second ($k = 1.979 \times 10^{-6}$ radian/sec).

Figure 18. - Precession of unit spin vector for 400-mile orbit initially normal to ecliptic plane with spin vector initially parallel to Earth's orbital velocity vector. Moment of inertia about spin axis, 385 slug-feet^2; moment of inertia about transverse axis, 264 slug-feet^2.

This condition results in a precession of the orbital plane about the polar axis. Although gravity gradient and oblateness effects are small in absolute magnitude, the fact that they can act continuously over a long period of time can make their net effect appreciable.

Analysis of Attitude Stability of Satellite

In order to evaluate passive attitude control of the proposed satellite for a 1-year lifetime, the assumption was made that all previously listed perturbation sources affecting the orbit and attitude of the satellite were of secondary importance with the exception of gravity-gradient torque and Earth oblateness. On the basis of these two perturbations, a study was made of the attitude behavior of the satellite for the sample mission previously discussed. All orbits studied were prograde.

Equations for the gravity gradient torque and its effect on satellite attitude are given in appendix C. The orbital geometry and the coordinate systems used in this discussion on satellite attitude are given in figure 15 (p. 19). For an Earth satellite, which is a body of revolution symmetric about

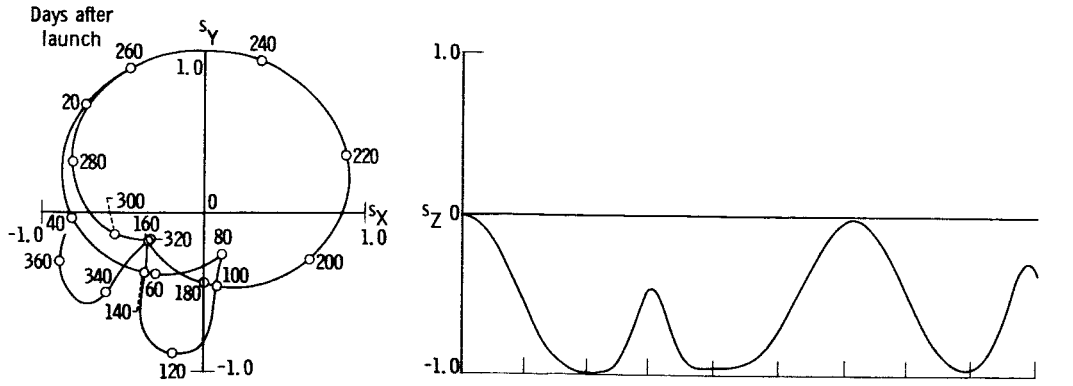

(c) Initial angular position of ascending node, 0^0; spin velocity of satellite, -0.549 radian per second ($k = -1.979 \times 10^{-6}$ radian/sec).

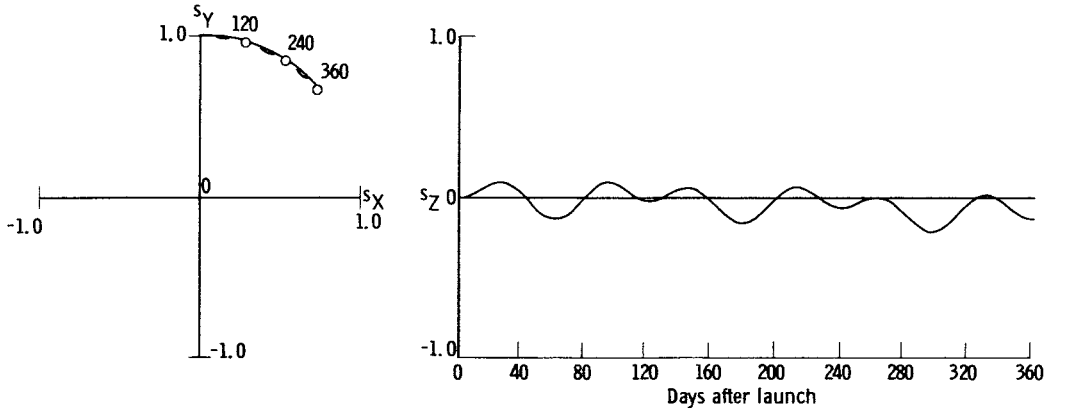

(d) Initial angular position of ascending node, 0^0; spin velocity of satellite, 2.195 radians per second ($k = 0.495 \times 10^{-6}$ radian/sec).

Figure 18. - Concluded. Precession of unit spin vector for 400-mile orbit initially normal to ecliptic plane with spin vector initially parallel to Earth's orbital velocity vector. Moment of inertia about spin axis, 385 slug-feet^2; moment of inertia about transverse axis, 264 slug-feet^2.

its spin axis, the instantaneous gravitational torque as presented in reference 5 is given by equation (C1) in appendix C. The average torque over one orbit as derived in reference 6 is presented in equation (C2). Either equation can be used with appropriate time increments to give essentially the same results for change in satellite attitude.

From equation (C1) or (C2) it is seen that if the satellite is spherically symmetric ($\Delta I = 0$) there is no gravitational gradient torque. Also, equation (C2) indicates that, if the spin axis is parallel or perpendicular to the orbital plane, the average torque over each orbit is approximately zero. This is not strictly true for the case in which the spin axis lies in the orbital plane because during an orbit continual slight changes in attitude produce unsymmetric conditions that are not accounted for in this approximation. In fact, as energy is dissipated, an Earth satellite tends to aline itself so that the axis of minimum moment of inertia is in the direction of the local vertical plane and the maximum moment of inertia axis is normal to the orbital plane (ref. 7). Unfortunately, even this orientation is not stable because of the oblateness of the Earth. This oblateness tends to precess the orbital plane about the polar axis of the Earth with a frequency that is a function of the mean altitude of the satellite and the orbital inclination angle (ref. 8).

Thus, even if the spin axis of the satellite is initially normal to the orbital plane, this orientation is not stable, except for polar and equatorial orbits.

The equations for the change in attitude brought about by gravity gradient torque and oblateness effects are presented in appendix C. These equations were programmed on an IBM 7094 electronic computer to obtain the longtime results presented in figures 16 to 19. Oblateness was accounted for simply by the nodal regression rate $d\Omega/dt$ as obtained from reference 8. For all cases shown in the figures, a 400-mile circular orbit was considered, and the spin vector was initially parallel to the Earth's orbital velocity vector and constant in magnitude. The left-hand sides of figures 16 to 19 represent the projection of the unit vector in the direction of the instantaneous-spin axis on the ecliptic plane. The right-hand sides give the component of the unit vector normal to the ecliptic plane as a function of time. Polar, equatorial, initially ecliptic, and initially normal to the ecliptic orbits are included in the study. Table I summarizes the input for the various computer solutions obtained. In most cases, a considerable amount of wandering of the spin axis takes place in the 1-year lifetime being considered. As is to be expected, the rate of precession is inversely proportional to the spin speed in all cases.

Polar orbits. - Some of the results for the polar orbit studies are shown in figure 16. The attitude of the spinning satellite is most stable and predictable in a polar orbit for the conditions investigated in this report. The motion is repetitious in that the direction of the spin vector is periodic in k (eq. (C7)). Therefore, the orbital altitude, spin speed, and mass distribution can be varied within limits, and the motion of the spin axis will be the same except for the time required for a change in attitude to take place. The attitude remains fixed for all practical purposes when the spin axis is parallel or perpendicular to the polar orbit plane. From the results not plotted in the figures because they would show only as a point, the case in which the spin

TABLE I. - INPUT DATA FOR IBM 7094 SATELLITE-ATTITUDE PROGRAM

Figure	Moment of inertia about spin axis, I_s, slug-ft^2	Moment of inertia about transverse axis, I_t, slug-ft^2	Geocentric angular velocity for circular orbit, ω_o, radians/sec (a)	Angle between orbital and equatorial planes, α, deg	Type of orbit	Initial angular position of ascending node, Ω_i, radians	Rate of change of angular position of ascending node, $\dot{\Omega}$, radians/sec	Instantaneous spin velocity of package, ω_s, radians/sec	Attitude parameter, k, radians/sec	Component of unit vector in X-direction at insertion into orbit, $s_{X,i}$	Component of unit vector in Y-direction at insertion into orbit, $s_{Y,i}$	Component of unit vector normal to ecliptic plane at insertion into orbit, $s_{Z,i}$
16(a)	385	264	0.001073	90	Polar	0	0	0.549	1.979×10^{-6}	0	1.000	0
16(b)	385	264	.001073	90	Polar	0	0	2.195	.495	0	1.000	0
17(a)	385	264	0.001073	0	Equatorial	---	1.455×10^{-6}	0.549	1.979×10^{-6}	0	1.000	0
17(b)	385	264	.001073	0	Equatorial	---	1.455	1.098	.989	0	1.000	0
17(c)	385	264	.001073	0	Equatorial	---	1.455	2.195	.495	0	1.000	0
18(a)	385	264	0.001073	66.5	Initially	0	0.588×10^{-6}	0.549	1.979×10^{-6}	0	1.000	0
18(b)	385	264	.001073	66.5	normal	$\pi/2$	.588	.549	1.979	0	1.000	0
18(c)	385	264	.001073	66.5	to	0	.588	-.549	-1.979	0	1.000	0
18(d)	385	264	.001073	66.5	ecliptic	0	.588	2.195	.495	0	1.000	0
19(a)	385	264	0.001073	23.5	Initially	0	1.331×10^{-6}	0.549	1.979×10^{-6}	0	1.000	0
19(b)	385	264	.001073	23.5	parallel	$\pi/2$	1.331	.549	1.979	0	1.000	0
19(c)	385	264	.001073	23.5	to ecliptic	0	1.331	2.195	.495	0	1.000	0

[a]Corresponds to 400-mile circular orbit.

axis was normal to the orbital plane was slightly more stable than that in which the spin axis lay in the orbital plane. Even in the worst of these cases, the attitude varied by less than 0.01 percent in 1 year for $\omega_s = 0.549$ radian per second which corresponds to $k = 1.979 \times 10^{-6}$ radian per second. (This attitude change was determined by projecting the final spin vector on its original position.) Consequently, if the attitude of the vehicle at any time is desired, and if active attitude control and attitude sensors are not incorporated into the design, a polar orbit with the spin axis parallel or perpendicular to the orbital plane enables one to predict the attitude quite accurately at any time. This prediction, of course, is based on the assumption that magnetic torques and other disturbances are small in comparison to the gravitational gradient torque. If the attitude in this polar orbit is established with the spin vector lying in the ecliptic plane, the sensing surface will periodically (every 6 months) be perpendicular to the Earth's orbital velocity vector and, thus, to the suspected path of most of the debris in the vicinity of the Earth. After 3 months of being out of phase with these periodic occurrences, the sensing surface will be parallel to the Earth's orbital velocity vector and should thus experience a minimum frequency of impact. Consequently, if the satellite has a sufficiently long lifetime, useful information as to the directionality of the impacting particles can be obtained.

If maintaining a suitable spin rate is not feasible, then a polar orbit, with the axis of symmetry normal to or in the orbital plane can be used where a stable attitude is desired because these orientations are inherently very stable even without spin.

Equatorial orbits. - Although a considerable amount of motion takes place in the equatorial orbit, it might be possible to use this motion to good advantage. There is reason to believe that if the spin axis of the satellite were to remain parallel to the Earth's orbital velocity vector, a maximum number of impacts would be experienced by the sensing surface within a given time (ref. 3). As seen in figure 17(b) (where $k = 0.989 \times 10^{-6}$ radian/sec), the spin axis precesses in such a way that it maintains the same general direction as the Earth's orbital velocity vector, although it does rise out of the ecliptic plane. As with the polar orbit, the motion is repetitious and periodic in k. In all except polar orbits, however, only the spin speed and mass distribution can be varied for a given value of k and still have the motion remain repetitious; this is because varying the altitude varies the oblateness effect, which is a function of orbital altitude and orbital inclination. Because the oblate Earth model used here is symmetric about the polar axis and the equatorial plane, the oblateness does not affect motion in polar orbits. Also, if the satellite is inserted into an equatorial orbit with its spin axis perpendicular to the orbital plane, its orientation will be stable. This can be done because the only effect of oblateness on equatorial orbits is to precess the apogee and perigee about the polar axis, the orbital plane always remaining parallel to its original position.

Initially normal to the ecliptic orbits. - Motion in an orbital plane that is initially normal to the ecliptic plane is shown in figure 18. Because of Earth oblateness, however, this plane varies with time between 43° and 90° to the ecliptic plane. The attitude behavior is much more erratic than was the case in either polar or equatorial orbits. As previously mentioned, the spin

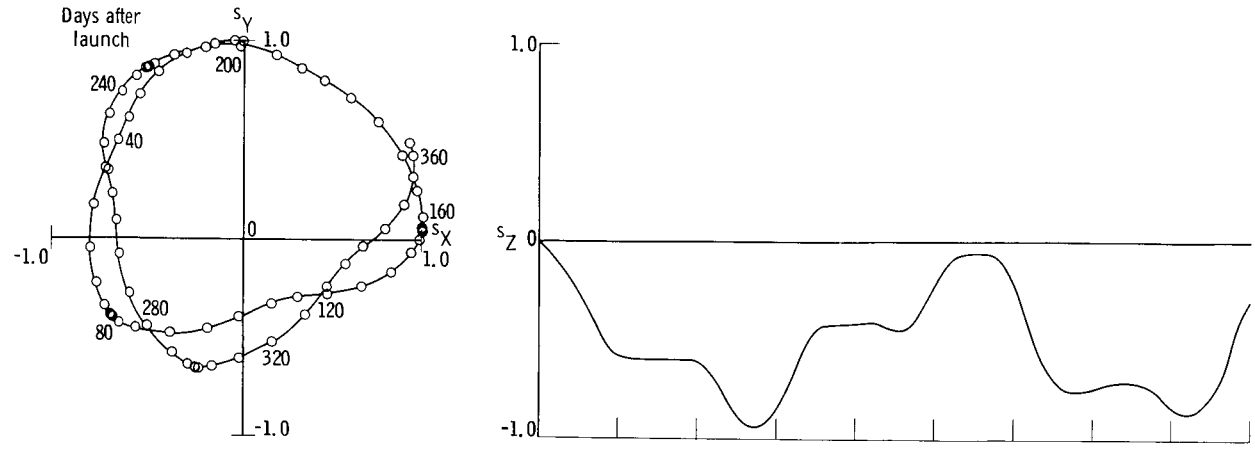

(a) Initial angular position of ascending node, 0^0; spin velocity of satellite, 0.549 radian per second ($k = 1.979 \times 10^{-6}$ radian/sec).

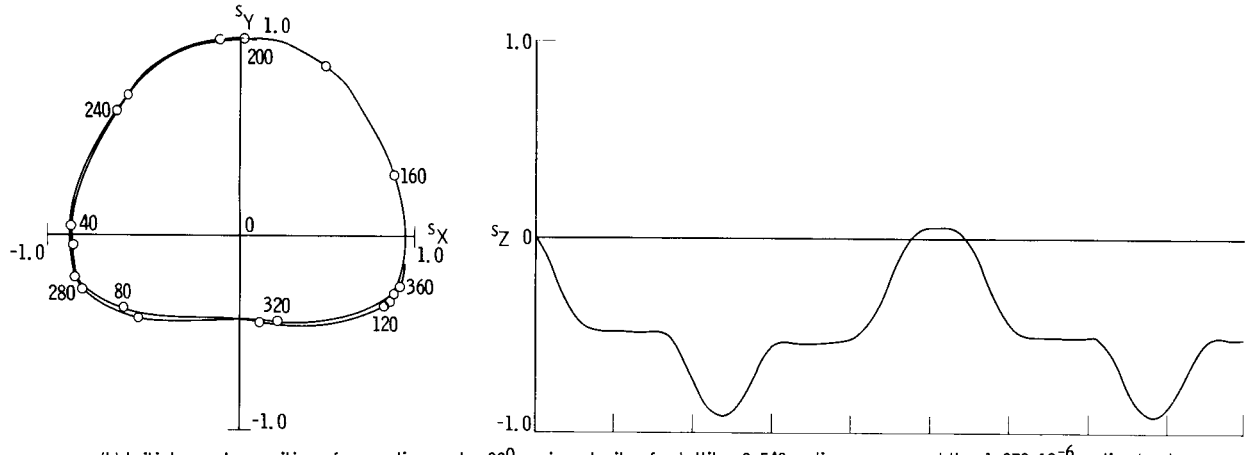

(b) Initial angular position of ascending node, 90^0; spin velocity of satellite, 0.549 radian per second ($k = 1.979 \times 10^{-6}$ radian/sec).

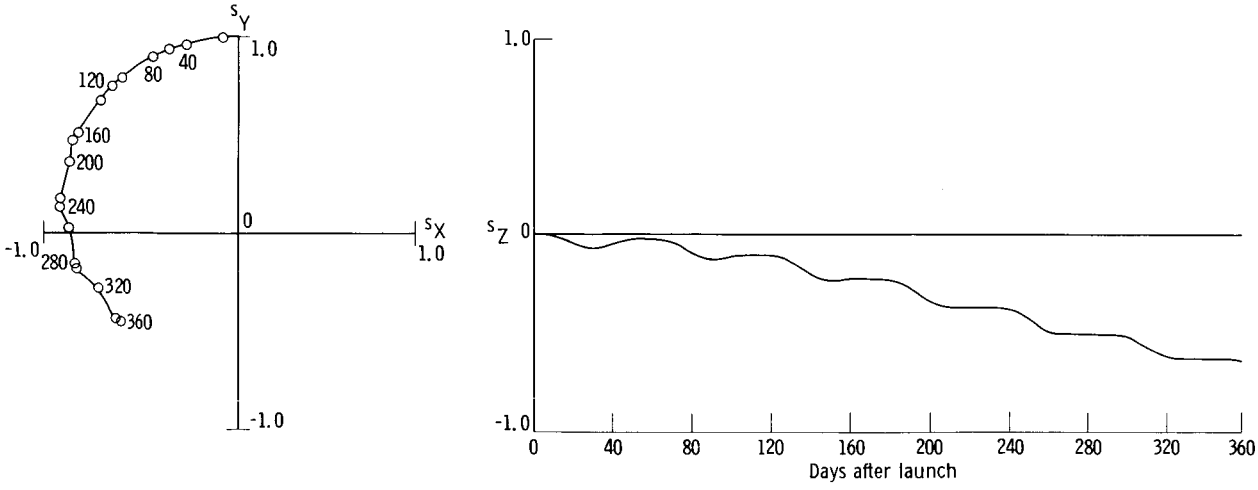

(c) Initial angular position of ascending node, 0^0; spin velocity of satellite, 2.195 radians per second ($k = 0.495 \times 10^{-6}$ radian/sec).

Figure 19. - Precession of unit spin vector for 400-mile orbit initially parallel to ecliptic plane with spin vector initially parallel to Earth's orbital velocity vector. Moment of inertia about spin axis, 385 slug-feet^2; moment of inertia about transverse axis, 264 slug-feet^2.

vector is initially parallel to the Earth's orbital velocity vector. The motion represented in figure 18(a) is for the case in which the spin axis is initially perpendicular to the orbital plane; that is, the orbital plane initially contains the Earth-Sun line. Figure 18(b) describes the motion when the spin axis originally lies in the orbital plane; thus, the orbital plane is initially normal to the Earth-Sun line. The initial conditions for the motion described in figure 18(c) are the same as for figure 18(a) except that the spin direction is reversed. The motions are obviously not very similar. This illustrates clearly a very significant point; namely, both the magnitude and direction of spin are very important in describing the motion of a spin-stabilized satellite. Figure 18(d) illustrates the motion when the spin speed is four times that for the motion described in figure 18(a). It can be seen that the satellite is much more stable with the higher spin rate.

Initially ecliptic orbits. - Finally, consideration was given to the motion in an initially ecliptic orbit plane (fig. 19). This plane varied with time from 0° to 47° with the ecliptic plane because of the oblateness of the Earth. As was the case with motion in a plane initially normal to the ecliptic, the motion is not repetitious, although it is not as erratic as was the motion in the plane normal to the ecliptic.

From the very few cases studied here for a 400-mile circular orbit of the Earth with the satellite spin vector initially parallel to the Earth's orbital velocity vector, the attitude of a spin-stabilized satellite may vary considerably. The examples presented herein are for purposes of illustration only. Many other combinations of the parameters listed in table I could be studied with the resulting attitude motions determined. From the examples considered, however, it is difficult to predict the attitude behavior of a satellite from a known but somewhat different case. Therefore, it was believed that little further general information could be obtained by studying more specific cases. More specific and extensive analyses of some of the more important factors affecting satellite attitude are presented in references 9 to 12.

CONCLUSIONS

Some general conclusions can be made from the studies described in this report as to configuration, stowage and deployment, and attitude stability of expandable spin-stabilized satellites.

Of the two basic configurations considered, the umbrella type is better than the wrap-around-wing type in a number of ways. Some of these ways are (1) the deployed umbrella satellite is stable about its original spin axis, whereas the wrap-around-wing satellite is not; (2) the maximum width dimension for a given test area is less for the umbrella satellite, which makes ground testing in space-environment facilities easier and decreases the length of the instrument leads connecting the sensors to the telemetry package; and (3) the deployment of the stowed umbrella package is more positively controlled. The main advantage of the wrap-around wing is compactness.

Two major factors affecting the design of the umbrella structure are the

initial spin rate and the method of deployment. Weight reductions possibly can be realized by using a lower initial spin rate on the last rocket stage before deployment.

Within the assumptions made for the attitude studies, a satellite in a polar orbit with its spin axis parallel or perpendicular to the orbital plane has an essentially stable attitude. Also, a satellite in an equatorial orbit having its spin axis normal to the orbital plane has a relatively stable attitude. All other cases considered resulted in precession of the spin axis of the satellite from its initial orientation, which was parallel to the Earth's orbital velocity vector. As would be expected, the rate of this precession was inversely proportional to the spin rate of the satellite in all cases. For the polar and equatorial orbits, the magnitude of the deviation from the initial orientation was independent of spin rate; for the initially ecliptic and normal to the ecliptic orbits, this magnitude was affected by the spin rate. In an equatorial orbit, the spin axis might possibly precess in such a way as to closely approximate the direction of the Earth's orbital velocity vector. The initially ecliptic and normal to the ecliptic orbits gave spin-axis orientations that were very erratic.

For an expandable spin-stabilized satellite the final choice of such design details as spin rate, deployment system, and nature of orbit, could be arrived at by making compromises based on the available payload envelope, launch vehicle requirements, experiment requirements, economic restrictions, and interactions of such environmental forces as gravity gradients and magnetic torques. The studies reported herein point out the effects of some of these factors that must be considered.

Lewis Research Center,
National Aeronautics and Space Administration,
Cleveland, Ohio, November 3, 1964.

APPENDIX A

SYMBOLS

C	velocity coefficient, ft
d	slider travel, ft
F	force, lb
G	dissipation function, equal to one-half the rate at which energy is dissipated, ft-lb/sec
I	moment of inertia, slug-ft^2
ΔI	difference between moments of inertia about the spin axis and transverse axis, $I_s - I_t$, slug-ft^2
KE	total kinetic energy, ft-lb
k	attitude parameter, $3\omega_o^2 \Delta I/\omega_s I_s$, radians/sec
l	distance from point 1, ft (fig. 10(b))
Δl_p	panel extension, ft
m	mass, slugs
N	number of degrees of freedom
Q_j	generalized forces corresponding to generalized coordinates describing motion
q_j	generalized coordinates describing motion
R	radial distance from spin axis of package, ft
$\vec{r}$	unit vector in direction of satellite position vector
$\vec{s}$	unit vector in direction of satellite spin axis
T_{gg}	gravitational gradient torque, lb-ft
t	time, sec or day
v	linear velocity, ft/sec
X,Y,Z	heliocentric ecliptic coordinate axes
x,y,z	geocentric equatorial coordinate axes

α	angle between orbital plane and equatorial plane, radians
β	angular position of satellite in orbit measured from ascending note in direction of motion, radians
θ	angular position about spin axis, radians
μ	damping coefficient, lb/(ft/sec)
φ	angular position of main support arm, radians
Ω	angular position of ascending node measured from x-axis, radians
ω_E	angular velocity of Earth about Sun, radians/sec
ω_o	geocentric angular velocity for circular orbit, radians/sec
ω_s	instantaneous spin velocity of satellite, radians/sec

Subscripts:

d	deployed
f	final
i	initial (at insertion into orbit)
k	nondeploying portion of satellite package
l	direction parallel to main support rod and tube
max	maximum
n	direction normal to rectangular panel surface
neg	negative
p	panel assembly and tube
pos	positive
r	main support rod
s	spin axis
t	transverse axis (normal to satellite spin axis)
u	undeployed (stowed)
X,Y,Z	heliocentric ecliptic coordinate axes
x,y,z	geocentric equatorial coordinate axes

θ direction tangent to circular arc about spin axis

φ about axis parallel to linkage pin 1

1 to 5 support linkage points (fig. 10(a))

Superscripts:

$\dot{}$ first derivative with respect to time

$\ddot{}$ second derivative with respect to time

$'$ first derivative with respect to φ

$\bar{}$ centroidal

$\vec{}$ vector quantity

APPENDIX B

ANALYSIS OF RESTRICTED SPIN DEPLOYMENT OF TELESCOPING-UMBRELLA SATELLITE

Equations of motion are developed in this appendix for restricted spin deployment of the umbrella satellite that is shown schematically in figures 10(a) and (b). The development of these equations is based on the following assumptions:

(1) Deployment takes place under conditions of zero gravity

(2) The mass center of the satellite is stationary

(3) The masses of rods A and B (fig. 7(c), p. 9) are negligible

(4) There is no friction

Damped Case

For a nonconservative dynamic system with constant potential energy and no external forces, the well-known Lagrangian equations are

$$\frac{d}{dt}\frac{\partial KE}{\partial \dot{q}_j} - \frac{\partial KE}{\partial q_j} + \frac{\partial G}{\partial \dot{q}_j} = 0 \qquad j = 1,N \tag{B1}$$

For the umbrella satellite, the generalized coordinates (fig. 10(b), p. 12) are

$$\left.\begin{aligned} q_{j=1} &= \theta \qquad \text{angular-spin coordinate} \\ q_{j=2} &= \varphi \qquad \text{angular-deployment coordinate} \end{aligned}\right\} \tag{B2}$$

The total kinetic energy is

$$KE = \frac{1}{2}\Big[m_r(v_{r,n}^2 + v_{r,l}^2 + v_{r,\theta}^2) + m_p(v_{p,n}^2 + v_{p,l}^2 + v_{p,\theta}^2) + m_k(v_{k,s}^2 + v_{k,\theta}^2) + (\bar{I}_{r,\varphi} + \bar{I}_{p,\varphi})\dot{\varphi}^2 + (\bar{I}_{r,\theta} + \bar{I}_{p,\theta} + \bar{I}_{k,\theta})\dot{\theta}^2\Big] \tag{B3}$$

The distance between the plane of the pivot points of the main support rods and the mass center of the satellite is

$$\bar{l} = \frac{(m_r l_r + m_p l_p)\cos\varphi + m_k l_k}{m_r + m_p + m_k}$$

Therefore, in accordance with assumption (2), the axial velocity of the satellite centerbody is

$$v_{k,s} = \dot{\bar{l}} = \frac{-(m_r l_r + m_p l_p)\sin\varphi + m_p l_p' \cos\varphi}{m_r + m_p + m_k}\dot{\varphi} \equiv C_{k,s} \times \dot{\varphi} \qquad \text{(B4a)}$$

in which

$$\dot{(\ )} = \frac{d(\ )}{dt} \quad \text{and} \quad (\ )' = \frac{d(\ )}{d\varphi}$$

The remaining velocity components of the various masses are

$$\left.\begin{aligned} v_{r,n} &= (l_r + C_{k,s}\sin\varphi)\dot{\varphi} \equiv C_{r,n} \times \dot{\varphi} \\ v_{r,l} &= -C_{k,s}\cos\varphi \times \dot{\varphi} \equiv C_{r,l} \times \dot{\varphi} \\ v_{r,\theta} &= (R_1 + l_r \sin\varphi)\dot{\theta} \equiv C_{r,\theta} \times \dot{\theta} \\ v_{p,n} &= (l_p + C_{k,s}\sin\varphi)\dot{\varphi} \equiv C_{p,n} \times \dot{\varphi} \\ v_{p,l} &= (l_p' - C_{k,s}\cos\varphi)\dot{\varphi} \equiv C_{p,l} \times \dot{\varphi} \\ v_{p,\theta} &= (R_1 + l_p \sin\varphi)\dot{\theta} \equiv C_{p,\theta} \times \dot{\theta} \\ v_{k,\theta} &= R_k\dot{\theta} \end{aligned}\right\} \qquad \text{(B4b)}$$

The moments of inertia of each support rod and panel about the centroidal axes and parallel to the spin axis are

$$\left.\begin{aligned} \bar{I}_{r,\theta} &= \bar{I}_{r,\varphi}\sin^2\varphi \\ \bar{I}_{p,\theta} &= \bar{I}_{p,n}\sin^2\varphi + \bar{I}_{p,l}\cos^2\varphi \end{aligned}\right\} \qquad \text{(B4c)}$$

The variations in the principal moments of inertia $\bar{I}_{p,n}$ and $\bar{I}_{p,l}$ during deployment are small and can be neglected. The variations in the dimensions l_p and d with the deployment angle φ are given in figure 10(c) for the sample problem linkage. Finally, for a linear-velocity viscous damper with coefficient μ, the dissipation function becomes

$$G = \frac{1}{2}\mu(v_{5,s} - v_{k,s})^2 = \frac{1}{2}\mu(d')^2\,\dot{\varphi}^2 \qquad \text{(B5)}$$

When equations (B1) to (B5) are combined, the equations of motion of the deploying umbrella satellite with viscous damping and no external forces are

$$\ddot{\theta}(m_r C_{r,\theta}^2 + m_p C_{p,\theta}^2 + m_k R_k^2 + \bar{I}_{r,\theta} + \bar{I}_{p,\theta} + \bar{I}_{k,\theta}) + \dot{\varphi}\dot{\theta}(2m_r C_{r,\theta} C'_{r,\theta} + 2m_p C_{p,\theta} C'_{p,\theta} + \bar{I}'_{r,\theta} + \bar{I}'_{p,\theta}) = 0 \qquad \text{(B6a)}$$

and

$$\ddot{\varphi}\left[m_r(C_{r,\varphi}^2 + C_{r,l}^2) + m_p(C_{p,\varphi}^2 + C_{p,l}^2) + m_k C_{k,s}^2 + \bar{I}_{r,\varphi} + \bar{I}_{p,\varphi}\right] + \dot{\varphi}^2\left[m_r(C_{r,\varphi}C'_{r,\varphi} + C_{r,l}C'_{r,l}) + m_p(C_{p,\varphi}C'_{p,\varphi} + C_{p,l}C'_{p,l}) + m_k C_{k,s} C'_{k,s}\right] - \frac{\dot{\theta}^2}{2}\left(2m_r C_{r,\theta} C'_{r,\theta} + 2m_p C_{p,\theta} C'_{p,\theta} + \bar{I}'_{r,\theta} + \bar{I}'_{p,\theta}\right) + \dot{\varphi}\left[\mu(d')^2\right] = 0 \qquad \text{(B6b)}$$

Equations (B6a) and (B6b) were integrated numerically, using a Ruge-Kutta procedure, to obtain the results shown in figures 11 to 13.

Fully Damped Deployment Case

For a dynamic system subjected to external forces, the right-hand sides of equations (B6a) and (B6b) are equal to generalized forces Q_j, which correspond to the generalized coordinates $q_{j=1} = \theta$ and $q_{j=2} = \varphi$. If the slider force $F_{5,s}$ is now considered as an external restraining force rather than an induced damping force, the generalized forces become

$$\left.\begin{aligned} Q_{j=1} &= 0 \\ Q_{j=2} &= -F_{5,s}d' \end{aligned}\right\} \qquad \text{(B7a)}$$

Fully damped or power-restrained deployment is assumed to take place slowly, which leads to the conditions

$$\ddot{\varphi} = \dot{\varphi} = 0 \qquad \text{(B7b)}$$

Equation (B6a) then vanishes, and equation (B6b), modified in accordance with

(B7a), leads to the following relation for the required restraining force:

$$F_{5,s} = \frac{m_r C_{r,\theta} C'_{r,\theta} + m_p C_{p,\theta} C'_{p,\theta}}{d} \dot{\theta}^2 \qquad \text{(B8a)}$$

The maximum restraining force is required when $\varphi = 0$, or

$$(F_{5,s})_{max} = \frac{m_r l_r + m_p l_p(0)}{d'(0)} R_1 \omega^2_{s,u} \qquad \text{(B8b)}$$

APPENDIX C

EFFECT OF GRAVITATIONAL TORQUE ON SATELLITE ATTITUDE

Reference 5 shows that the instantaneous gravitational gradient torque acting on an Earth satellite is

$$T_{gg} = 3\omega_o^2 \Delta I(\vec{r} \cdot \vec{s})(\vec{r} \times \vec{s}) \tag{C1}$$

The average torque over one orbit is (ref. 6)

$$(T_{gg})_{ave} = -\frac{3}{2} \Delta I(\vec{\omega}_o \cdot \vec{s})(\vec{\omega}_o \times \vec{s}) \tag{C2}$$

By using the classical equation for gyroscopic motion, a very direct approach for determining the attitude of a spinning satellite acted on by gravitational torque is presented in reference 2. The equation relating the rate of change in attitude to the gravitational torque is

$$I_s \omega_{s,d} \frac{d\vec{s}}{dt} = T_{gg} \tag{C3}$$

By substituting either equation (C1) or (C2) into equation (C3) and by using appropriate time increments, the change in attitude of the spin axis due to gravitational torque can be found. Since the initial attitude is a known quantity, the attitude at any time can now be obtained.

As was shown in reference 2, substitution of equation (C1) into equation (C3) results in

$$\frac{ds_x}{dt} = k(r_x s_x + r_y s_y + r_z s_z)(r_y s_z - r_z s_y) \tag{C4}$$

$$\frac{ds_y}{dt} = k(r_x s_x + r_y s_y + r_z s_z)(r_z s_x - r_x s_z) \tag{C5}$$

$$\frac{ds_z}{dt} = k(r_x s_x + r_y s_y + r_z s_z)(r_x s_y - r_y s_x) \tag{C6}$$

where

$$k = 3 \frac{\omega_o^2}{\omega_s} \frac{\Delta I}{I_{s,d}} \tag{C7}$$

The geocentric equatorial coordinate system to which the unit vector $\vec{s}$ is herein referred is shown in figure 15(a) (p. 19). The vector $\vec{s}$ can also be referred to the heliocentric ecliptic coordinate system shown in figure 15(b) by the equations

$$s_X = s_x \tag{C8}$$

$$s_Y = s_y \cos 23.5^\circ - s_z \sin 23.5^\circ \tag{C9}$$

$$s_Z = s_y \sin 23.5^\circ + s_z \cos 23.5^\circ \tag{C10}$$

The results presented in figures 16 to 19 (pp. 20 to 26) refer to the ecliptic coordinate system.

The position of the satellite with respect to the Earth at any time (see fig. 15(a)) is given by

$$r_x = \cos \Omega \cos \beta + \sin \Omega \sin \beta \cos \alpha \tag{C11}$$

$$r_y = \sin \Omega \cos \beta - \cos \Omega \sin \beta \cos \alpha \tag{C12}$$

$$r_z = \sin \beta \sin \alpha \tag{C13}$$

The effect of Earth oblateness on the attitude of a spin-stabilized Earth satellite is accounted for simply by a change in the position of the ascending node Ω. The oblateness tends to precess the orbital plane about the Earth's polar axis periodically as a function of orbital altitude and inclination angle. A plot of nodal regression rate as a function of mean altitude and orbital inclination angle is given in reference 8.

REFERENCES

1. Anon.: Sunflower Solar Collector. Topical Rep. ER-5555, Thompson-Ramo Wooldridge, Inc., Sept. 1963.

2. Grasshoff, L. H.: Influence of Gravity on Satellite Spin Axis Attitude. ARS Jour., vol. 30, no. 12, Dec. 1960, pp. 1174-1175.

3. Davison, Elmer, H., and Winslow, Paul C., Jr.: Space Debris Hazard Evaluation. NASA TN D-1105, 1961.

4. Holahan, James: Attitude Control for Unmanned Spacecraft. Space/ Aeronautics, vol. 39, no. 2, Feb. 1963, pp. 78-86.

5. Nidey, Russell A.: Gravitational Torque on a Satellite of Arbitrary Shape. ARS Jour., vol. 30, no. 2, Feb. 1960, pp. 203-204.

6. Nidey, Russell A.: Secular Gravitational Torque on a Satellite in a Circular Orbit. ARS Jour., vol. 31, no. 7, July 1961, p. 1032.

7. Kamm, Lawrence J.: "Vertistat": An Improved Satellite Orientation Device. ARS Jour., vol. 32, no. 6, June 1962, pp. 911-913.

8. Jensen, J., Townsend, G., Kork, J., and Kraft, D.: Design Guide to Orbital Flight. McGraw-Hill Book Co., Inc., 1962, p. 166.

9. Doolin, Brian F., and Triplett, William C.: The Influence of Gravity on the Angular Motion of an Earth Satellite. Advances in Astronautical Sci., vol. 6, Macmillan Co., 1961, pp. 524-535.

10. Naumann, Robert J.: Observed Torque-Producing Forces Acting on Satellites. NASA TR R-183, 1963.

11. Yu, E. Y.: Spin Decay, Spin-Precession Damping, and Spin-Axis Drift of the Telstar Satellite. Bell System Tech. Jour., vol. 42, no. 5, Sept. 1963, pp. 2169-2193.

12. Patapoff, Harry: Attitude Drift of a Spin Stabilized Satellite Due to the Earth's Magnetic and Gravitational Fields. Paper 66, Presented at XIV Int. Astronautical Cong., Paris (France), Sept. 25-Oct. 1, 1963.

NASA-Langley, 1965 E-2234